



1 **Does the GPM mission improve the systematic error component in satellite**
2 **rainfall estimates over TRMM, an evaluation at a pan-India scale?**

3 Harsh Beria¹, Trushnamayee Nanda¹, Deepak Singh Bisht¹, Chandranath Chatterjee¹

4 ¹Agricultural and Food Engineering Department, Indian Institute of Technology Kharagpur,
5 Kharagpur, India

6 *Correspondence to:* Harsh Beria (harsh.beria93@gmail.com)

7 **Abstract.** Last couple of decades have seen the outburst of a number of satellite based
8 precipitation products with Tropical Rainfall Measuring Mission (TRMM) as the most widely
9 used for hydrologic applications. Transition of TRMM into Global Precipitation Mission
10 (GPM) promises enhanced spatio-temporal resolution along with upgrades in sensors and
11 rainfall estimation techniques. Dependence of systematic error components in rainfall
12 estimates of Integrated Multi-satellitE Retrievals for GPM (IMERG), and their variation with
13 climatology and topography, was evaluated over 86 basins in India for year 2014 and
14 compared with the corresponding (2014) and retrospective (1998-2013) TRMM estimates.
15 IMERG outperformed TRMM for all rainfall intensities across a majority of Indian basins,
16 with significant improvement in low rainfall estimates showing smaller negative biases in 75
17 out of 86 basins. IMERG increased the inter-basin variability in bias for medium and high
18 rainfall estimates. Low rainfall estimates in TRMM showed a systematic dependence on
19 basin climatology, with significant overprediction in semi-arid basins which gradually
20 improved in the higher rainfall basins. Medium and high rainfall estimates of TRMM
21 exhibited a strong dependence on basin topography, with declining skill in the higher
22 elevation basins. Systematic dependence of error components on basin climatology and
23 topography was reduced in IMERG, especially in terms of topography. Rainfall-runoff
24 modeling using Variable Infiltration Capacity (VIC) model over a flood prone basin
25 (Mahanadi) revealed that improvement in rainfall estimates in IMERG didn't translate into
26 improvement in runoff simulations. More studies are required over basins in different hydro-
27 climatic zones to evaluate the hydrologic significance of IMERG.

28 **Keywords:** GPM, IMERG, TRMM, VIC, climatology, topography



29 **1 Introduction**

30 The developing part of the world suffers from acute data shortage, both in terms of
31 quality and quantity. A recent commentary from Mujumdar (2015) provided insights into the
32 problems faced by the Indian hydrologic community due to the lack of willingness of the
33 relevant governmental bodies to openly share meteorologic and hydrologic data and its meta
34 data to the research community. With the threats of climate changing looming large, high
35 quality precipitation products (in terms of accuracy, spatial and temporal resolution) are the
36 need of the hour. Satellite precipitation products offer a viable alternative to gauge based
37 rainfall estimates.

38 A number of satellite based precipitation estimates have cropped up in the past two
39 decades, the famous ones being Climate Prediction Center morphing technique (CMORPH),
40 Precipitation Estimation from Remotely Sensed Information Using Artificial Neural
41 Networks (PERSIANN), PERSIANN Climate Data Record (PERSIANN-CDR), Tropical
42 Rainfall Measuring Mission (TRMM), Asian Precipitation - Highly-Resolved Observational
43 Data Integration Towards Evaluation (APHRODITE) and National Oceanic and Atmospheric
44 Administration (NOAA) Climate Prediction Center (CPC). A number of studies over the past
45 decade have evaluated the hydrologic application of these datasets over regions with varied
46 topography and climatology.

47 Artan et al. (2007) used CPC to drive a hydrologic model over four basins with varied
48 hydro-climatic and physiographic conditions in Africa and South-east Asia and reported
49 similar rainfall-runoff performance on calibration using gauge and satellite rainfall estimates.
50 Collischonn et al. (2008) also reported reasonable streamflow simulations using TRMM
51 estimates over an Amazon River basin. Akhtar et al. (2009) used multiple artificial neural
52 networks (ANN) to forecast discharges at varying lead times using TRMM 3B42V6
53 precipitation estimates. Wu et al. (2012) used TRMM 3B42V6 estimates to develop a real-
54 time flood monitoring system and concluded that the probability of detection (POD)
55 improved with longer flood durations and larger affected areas. Kneis et al. (2014) evaluated
56 TRMM 3B42-V7 and its real-time counterpart TRMM 3B42-V7RT over Mahanadi River
57 basin in India and found the research product (3B42) to be superior to the real-time
58 alternative (3B42RT) in terms of both the statistical and hydrologic components. Peng et al.
59 (2014) found a systematic dependence of TRMM estimates on climatology in North-West
60 China, characterizing the wetter regions better than the drier conditions. They also reported



61 promising results in the streamflow simulations at ungauged basin in arid and semi-arid
62 regions. Bajracharya et al. (2014) used CPC to drive a hydrologic model over Bagmati basin
63 in Nepal and reported that the incorporation of local rain gauge data in addition to CPC
64 tremendously benefited the streamflow simulations. Shah and Mishra (2015) explored the
65 uncertainty in the estimates of multiple satellite rainfall products over major Indian basins
66 and investigated the influence of bias in the satellite rainfall products on flood simulation
67 over Mahanadi River basin in India. Most of the studies which evaluated multiple satellite
68 precipitation estimates have reported TRMM to give the best estimate over the Tropical part
69 of the world (Gao and Liu, 2013; Prakash et al., 2016b; Zhu et al., 2016).

70 Tropical Rainfall Measuring Mission (TRMM) satellite was launched in late 1997 and
71 provides high resolution ($0.25^\circ \times 0.25^\circ$) quasi-global (50° N-S) rainfall estimates (Huffman et
72 al., 2007). The TRMM mission is a joint mission between the National Aeronautics and
73 Space Administration (NASA) and the Japan Aerospace Exploration (JAXA) Agency to
74 study rainfall for weather and climate research. The TRMM satellite produced 17 years of
75 valuable precipitation data over the Tropics. In the last decade, a number of studies have
76 evaluated Tropical Rainfall Measuring Mission (TRMM) Multi-Resolution Analysis (TMPA)
77 product over different topographies and climatologies.

78 Owing to the tremendous success of TMPA mission, Global Precipitation
79 Measurement (GPM) was launched on February 27, 2014 (Liu, 2016). The GPM sensors
80 carry first spaceborne dual-frequency phased array precipitation radar (DPR) operating at Ku
81 (13 GHz) and Ka (35 GHz) bands and a canonical-scanning multichannel (10 - 183 GHz)
82 microwave imager (GMI) (Hou et al., 2014). The improved sensitivity of Ku and Ka bands
83 allow for improved detection of low precipitation rates (<0.5 mm/h) and falling snow.

84 A few preliminary assessments of GPM over India and China (Prakash et al., 2016a,
85 2016b; Tang et al., 2016a) suggest an improvement over TMPA. For 2014 monsoon (Prakash
86 et al., 2016b) reported that Integrated Multi-satellitE Retrievals for GPM (IMERG), which is
87 a level three multi-satellite precipitation algorithm of GPM (Hou et al., 2014), outperformed
88 TMPA in extreme rainfall detection along the Himalayan foothills in North India and over
89 North Western India, with slightly reduced false alarms. Tang et al. (2016a) found that
90 IMERG outperformed TMPA in almost all the indices for every sub-region of mainland
91 China at 3-hourly and daily temporal resolutions. They also reported that IMERG reproduced
92 probability density functions more accurately at various precipitation intensities and better



93 represented the precipitation diurnal cycles. In another work by Prakash et al. (2016a),
94 IMERG was compared with Global Satellite Mapping of Precipitation (GSMaP) V6 and
95 TMPA 3B42V7 for the 2014 monsoon over India. It was found that IMERG estimates
96 represented the mean monsoon rainfall and its variability more realistically, with fewer
97 missed and false precipitation bias and improvements in the precipitation distribution over
98 low rainfall rates.

99 Most of the previous studies that compared satellite and reanalysis precipitation
100 products for pan-India focused at a grid scale, rather than a basin scale (Prakash et al., 2015,
101 2016a, 2016b). We focused at a basin scale as it is more relevant in terms of water resources
102 assessment for policy makers. Also, it provides a clear signal of the utility of the satellite
103 precipitation products at the required spatial resolution for water managers working at a basin
104 scale.

105 In this study, we comprehensively evaluated TRMM 3B42 from 1998-2013 over 86
106 basins in India and explored systematic biases due to climatology and topography. We then
107 compared TRMM 3B42 precipitation estimates with IMERG for 2014 and explored if the
108 systematic biases were reduced in IMERG, and whether IMERG was able to better capture
109 the low rainfall magnitudes. Finally, we used a macroscale hydrologic model (Variable
110 Infiltration Capacity (VIC)) to evaluate TRMM and IMERG over a flood prone basin in
111 Eastern India (Mahanadi River basin) for the year 2014.

112 **2 Description of the study area, datasets used and methodology**

113 **2.1 Study area**

114 The study was conducted over India at a basin scale (Fig. 1a). Water Resources
115 Information System of India (India-WRIS) divides India into 91 major basins (India, 2014).
116 In this study, 86 basins were used, with the five excluded basins located in the Jammu and
117 Kashmir region of Northern India (details included in Supplementary table 1). Also, the
118 Lakshadweep islands (located off the Indian West coast in the Arabian Sea) and the Andaman
119 and Nicobar islands (located in the Bay of Bengal) were excluded from the analysis due to
120 scanty rain-gauge monitoring network.

121 Most of India experiences a tropical monsoon type of climate receiving an average
122 annual rainfall of around 1100 mm/year, of which about 70-80% is concentrated during the
123 monsoon season (June – September). Fig. 1b shows the spatial distribution of rainfall,



124 calculated using India Meteorological Department (IMD) gridded precipitation dataset
125 (computed using 31 years (1980-2010) of rainfall time series) over India. The Western Ghats
126 (located on the Indian West coast) and the North-Eastern basins receive the highest rainfall,
127 with the magnitude going as high as 3000 mm/year. The Western Ghats receive orographic
128 rainfall due to the steep topographic gradient that exist from the West to the East, making the
129 Eastern part of the mountains a leeward area where rainfall is mainly associated with the
130 passage of lows and depressions developed in the Bay of Bengal (Prakash et al., 2016a).
131 Details of the orographic features of rainfall over Western Ghats can be found in Tawde and
132 Singh (2015). The high rainfall in the North-Eastern part of India is associated with
133 orographic control and multi-scale interactions of monsoon flow (Prakash et al., 2016a).
134 Basins in the Indo-Gangetic plain and on the East coast receive above average rainfall of
135 around 1400 mm/year, governed by the tropical monsoons. The hilly tracts of Jammu and
136 Kashmir situated in North-most part of India receive an annual average rainfall of around
137 1000 mm/year. The North-west basins, associated with semi-arid type of climate, receive low
138 annual rainfall ranging from 300-400 mm/year. The basin-wise rainfall is provided in
139 Supplementary table 1.

140 Fig. 1c shows the spatial distribution of the basin-wise elevation above mean sea level
141 (m.s.l). The Northern tract of Jammu and Kashmir comprises the basins with highest
142 elevations, in between 2500 m to 5000 m above m.s.l. These basins also suffer from scanty
143 rain monitoring networks, due to which five of these high elevation basins have been ignored
144 in the analysis (details in Supplementary table 1). High Pitch Mountains are also found in the
145 North-Eastern basins where basin-wise elevation goes as high as 1400 m above m.s.l. The
146 Western Ghats are characterized by a very sharp topographic gradient with the elevations
147 increasing from around 200 m on the West coast to above 600 m above m.s.l as we move
148 east. This transition results in heavy orographic rainfall on the West coast and leads to the
149 sharp rainfall contrast on the leeward side of the Western Ghat Mountains. The Indo-
150 Gangetic plain and the Eastern basins are mostly plateau areas, with basin elevation lying in
151 between 200-400 m above m.s.l. The semi-arid North-Western basins are also characterized
152 by plateau land (elevation between 200-300 m above m.s.l). The basin-wise elevation is
153 provided in Supplementary table 1.

154 The rainfall-runoff modeling exercise was carried out in the Hirakud catchment of the
155 Mahanadi River basin (MRB), located on the Eastern coast of India. MRB is one of the
156 largest Indian basins draining an area of 1,41,000 km², mostly flowing through the states of



157 Chattisgarh and Odisha. It is prone to frequent flooding at the downstream, with five major
158 flood events in the first decade of the 21st century (Jena et al., 2014). On the upstream of the
159 MRB is a multi-purpose dam (Hirakud) which encompasses catchment area of around 85,200
160 km² and spans between 19.5° and 23.8° N latitudes and 80° to 84° E longitudes (Fig. 1d).
161 Hirakud dam started its operations in 1957 and its upstream does not include any major dam,
162 although a number of small scale irrigation reservoirs are operational during the monsoon.
163 The area experiences a tropical monsoon type of climate, with an annual rainfall of around
164 1500 mm. Agricultural, forest and shrub land account for around 55%, 35% and 7% of the
165 total basin coverage respectively (Kneis et al., 2014).

166 2.2 Datasets used

167 IMD gridded rainfall dataset was used as the reference product and Tropical Rainfall
168 Measuring Mission (TRMM) and Integrated Multi-satellitE Retrievals for GPM (IMERG)
169 were compared against IMD. A brief summary of the datasets is given in Table 1. A brief
170 introduction to the three rainfall datasets is given below.

171 2.2.1 Gridded IMD and streamflow dataset

172 IMD gridded precipitation dataset provides daily rainfall estimates over the Indian
173 landmass from 1901-2014 at a spatial resolution of 0.25° x 0.25°. It has been developed using
174 a dense network of rain gauges consisting of 6955 stations and is known to reasonably
175 capture the heavy orographic rainfall in the Western Ghats, the Northeast and the low rainfall
176 on the leeward side of the Western Ghats. For a detailed discussion on the evolution of IMD
177 gridded dataset, refer to Pai et al. (2014).

178 It is to be noted that IMD measures rainfall accumulation at 8:30 AM Indian Standard
179 time (IST) or (3:00 AM UTC). The accumulated rainfall for the previous day is provided as
180 the rainfall estimate for current day. For instance, IMD rainfall estimate at a gauging station
181 for September 14th, 2014 refers to the rainfall accumulation from 8:30 AM IST (3:00 AM
182 UTC) on September 13th, 2014 to 8:30 AM IST (3:00 AM UTC) on September 14th, 2014.
183 Both TRMM and IMERG precipitation estimates were converted to IMD timescale.

184 The gridded daily minimum and maximum temperature was obtained from IMD at a
185 spatial resolution of 1° x 1° (Srivastava et al., 2009). Daily wind speed data was obtained
186 from coupled National Centers for Environmental Prediction (NCEP) and Climate Forecast
187 System Reanalysis (CFSR) at a spatial resolution of 0.5° x 0.5°. Daily discharge data at the



188 inflow site of the Hirakud reservoir was obtained from the State Water Resources Department
189 (Odisha), Hirakud Dam Project, Burla, Sambalpur.

190 **2.2.2 Tropical Rainfall Measuring Mission (TRMM)**

191 In order to provide high resolution precipitation dataset in real-time, the TRMM
192 satellite was launched in late 1997 and it provides 3-hourly rainfall estimates from 1998 to
193 the current date at a quasi-global coverage (50° N-S) at a spatial resolution of 0.25° x 0.25°
194 (Huffman et al., 2007). Two variants of TRMM multi-satellite precipitation analysis (TMPA)
195 are available, a real time product which is available at 3-6 hours latency and the research
196 product which is available at 2-months latency. TRMM research product makes use of rain
197 gauge stations from Global Precipitation Climatology Centre (GPCC) to post-process the
198 TRMM estimates, details of which can be found in Huffman et al. (2007). We used TRMM
199 research product in this study (henceforth mentioned as TRMM).

200 **2.2.3 Integrated Multi-Satellite Retrievals for GPM (IMERG)**

201 Due to the great success of TMPA mission, Global Precipitation Measurement (GPM)
202 was launched on February 27, 2014 (Liu, 2016). IMERG is the day-1 multi-satellite
203 precipitation algorithm for GPM which combines data from TMPA, PERSIANN, CMORPH
204 and NASA PPS (Precipitation Processing System). For a detailed understanding of the
205 retrieval algorithm of IMERG, refer to (Huffman et al., 2014; Liu, 2016).

206 The major advancement in GPM satellite is the improved sensitivity of sensors
207 leading to improved detection of low precipitation rates (<0.5 mm/h) and falling snow, a
208 known shortcoming of TRMM. IMERG is available in 3 variants, (a) Early run (latency ~ 6
209 hours), (b) Late run (latency ~ 18 hours) and (c) Final run (latency ~ 4 months) (Liu, 2016).
210 Each product is available at half-hourly temporal and 0.1° x 0.1° spatial resolution. The
211 spatial coverage is 60° N-S which is planned to be extended to 90° N-S in the near future. We
212 used the Final run product in our analysis.

213 **2.3 VIC Hydrological Model**

214 VIC is a macroscale semi-distributed hydrological model which uses a grid-based
215 approach to quantify different hydro-meteorological processes by solving water balance and
216 energy flux equations, specifically designed to represent the surface energy and hydrologic
217 fluxes at varying scales (Liang et al., 1994, 1996). VIC uses multiple soil layers with variable



218 infiltration, non-linear baseflow and addresses the sub-grid scale variability in vegetation. A
219 stand-alone routing model (Lohmann et al., 1996) is used to generate runoff and baseflow at
220 the outlet of each grid cell, assuming linear and time-invariant runoff transport. The land
221 surface parameterization (LSP) of VIC is coupled with a routing scheme in which the
222 drainage system is conceptualized by connected-stem rivers at a grid scale. The routing
223 model extends the FDTF-ERUHDIT (First Differenced Transfer Function-Excess Rainfall
224 and Unit Hydrograph by a Deconvolution Iterative Technique) approach (Duband et al.,
225 1993) with a time scale separation and liberalized Saint-Venant equation type river routing
226 model. The model assumes runoff transport process to be linear, stable and time invariant.

227 VIC has been successfully used in a number of global and local hydrologic studies
228 (Hamlet and Lettenmaier, 1999; Shah and Mishra, 2015; Tong et al., 2014; Wu et al., 2014;
229 Yong et al., 2012). A recent commentary on the need for process-based evaluation of large-
230 scale hyper-resolution models by Melsen et al. (2016) provides interesting insights into the
231 use of VIC at different spatial scales and why we shouldn't just decrease the grid size (hence
232 increasing the spatial resolution of model) without considering the dominant processes at that
233 scale. In lines with the discussions in Melsen et al. (2016), VIC was run at a grid size of 0.5°
234 $\times 0.5^\circ$.

235 **2.4 Methodology**

236 All the analysis was performed at a basin scale. Basin-wise mean areal rainfall was
237 calculated for all the three rainfall products (IMD, TRMM and IMERG) using Thiessen
238 Polygon method for their respective periods of availability.

239 In order to statistically evaluate the precipitation products, two skill measures were
240 used (Pearson correlation (R) and percentage bias (Pbias/bias)) along with two threshold
241 statistics (probability of detection (POD) and false alarm ratio (FAR)). Table 2 shows the
242 contingency table and Table 3 provides a summary of the statistical indices.

243 All the statistical inferences were drawn for the overall time series, and then
244 separately for the different rainfall regimes. Table 4 shows the criterion to segregate the
245 rainfall time series into different components. For computing POD and FAR for different
246 rainfall regime, a threshold is required. The 25th percentile value was selected as the
247 threshold for low rainfall regime, 50th percentile for medium regime, 75th percentile for high



248 rainfall regime and 95th percentile for very high rainfall regime. The statistical indices were
249 calculated basin-wise.

250 In order to identify systematic bias in the satellite products, one meteorologic index
251 (long term basin mean annual rainfall) and one topographic index (basin mean elevation) was
252 computed for the 86 basins. The long term mean annual rainfall was computed using IMD
253 gridded dataset from 1980 – 2010 (31 years). Basin mean digital elevation model (DEM) was
254 extracted from Shuttle Radar Topography Mission (SRTM) DEM and mean elevation was
255 obtained on a basin-wise scale.

256 Due to the limited availability of IMERG data (starting from 2014), calibration of
257 VIC was done using an approach similar to the one used by Tang et al. (2016b). First, VIC
258 was calibrated (2000-2011) and validated (2011-2014) using gridded IMD precipitation time
259 series. VIC was then calibrated (2000-2011) and validated (2011-2014) with TRMM
260 precipitation time series. Further, both the IMD and TRMM calibrated models were validated
261 with IMERG and TRMM for the year 2014 (from April 1, 2014 to December 31st, 2014).
262 The year 2000 was used as a warm up period for the model.

263 In line with the recent discussion by McCuen (2016) on the correct usage of statistical
264 and graphical indices to evaluate model calibration and validation, four statistical parameters
265 (Nash Sutcliffe efficiency (NSE), Percentage bias (Pbias), coefficient of determination (R^2)
266 along with its significance probability (p-value) and root mean squared error (RMSE)) were
267 used to evaluate the runoff simulations from VIC. Table 3 provides a summary of these
268 indices.

269 **3 Results**

270 All the TRMM statistics were obtained for two distinct periods (1998-2013 and
271 2014). For the year 2014, the IMERG precipitation estimates were available from March 12,
272 2014. Therefore, the TRMM statistics for the year 2014 were obtained from March 12, 2014
273 to December 31, 2014. Henceforth, for the sake of convenience, statistics of TRMM-R refers
274 to the time period 1998-2013, statistics of TRMM and IMERG refers to the time period
275 March 12, 2014 to December 31, 2014.

276 **3.1 Scatterplots**



277 Fig. 2.1 shows the scatterplot of IMERG and TRMM with respect to IMD
278 precipitation combining data from all the 86 basins for the year 2014. Both IMERG and
279 TRMM show quite similar skills with correlation values above 0.8, with IMERG showing
280 better correlation in 60 out of 86 basins. On looking at the scatterplots for individual basins
281 (Fig. 2.2), IMERG tends to be better correlated to IMD than TRMM. It can be seen that the
282 correlation values go as high as 0.96 for IMERG (and 0.94 for TRMM) with a very uniform
283 spread across the 1:1 line for the five best basins (Figs. 2.2a–e) (decided on the basis of
284 correlation of IMERG with IMD in 2014). These basins are situated in the flat Deccan
285 Plateau belt in South-central India (mostly concentrated in Tapi and Godavari basins). For
286 the other five basins (Figs. 2.2f–j), the poor correlation is due to the gross overestimation of
287 IMERG/TRMM over IMD. Four of these five basins are situated in the high elevation basins
288 in Northern India, which hints at a systematic dependence of IMERG/TRMM estimates with
289 elevation. This is explored in detail in section e.

290 3.2 Basin-wise correlation

291 Basin-wise correlation was computed for retrospective analysis of TRMM-R and to
292 compare TRMM and IMERG rainfall estimates for the year 2014. Fig. 3 suggests that
293 IMERG gives slightly better rainfall estimate than TRMM for all rainfall regimes (with
294 IMERG showing higher correlation for the year 2014 for 60, 52, 52 and 55 out of 86 basins
295 for overall, low, medium and high rainfall regimes). IMERG shows a correlation coefficient
296 higher than 0.8 (for overall time series) for 73 out of 86 basins, compared to 68 basins for
297 TRMM and higher than 0.9 for 20 basins compared to 13 for TRMM. The decomposition of
298 the overall time series into different rainfall regime reduces the correlation, which can be
299 attributed to temporal smoothening in longer time series.

300 The spatial maps (Fig. 4) provide an illustration of the slight improvement of IMERG
301 over TRMM with spatially coherent patterns. In general, both TRMM and IMERG show high
302 basin-wise correlation values for the overall time series. In the overall spatial maps (Figs. 4b–
303 c), for the year 2014, TRMM and IMERG show similar skill, with IMERG capturing the
304 rainfall slightly better in Central and Southern India. Both show similar skill in the high
305 rainfall areas of the Western Ghats and the North Eastern basins. IMERG gives slightly better
306 estimates in the high elevation basins in North India. There is no significant improvement in
307 the basins located on the Eastern coast (like the Mahanadi river basin). TRMM provides
308 slightly better estimates of rainfall in the semi-arid basins located in the North Western states



309 of India (Rajasthan). It is to be noted that TRMM statistics for 2014 are much better than its
310 retrospective statistics (TRMM-R) with spatial coherent trends.

311 The low rainfall estimates (Figs. 4d–f) over the semi-arid North Western basins are
312 slightly better for TRMM compared to IMERG. IMERG captures low rainfall better over the
313 Indo-Gangetic plain. Both IMERG and TRMM show similar trends over the Western Ghats,
314 North-Eastern basins, Eastern coast and over the Deccan Plateau. IMERG doesn't capture the
315 low rainfall regime over the Upper Indus basin (in Northern India) and over the upper Bhima
316 and the upper Godavari basin (in the Deccan plateau belt).

317 The medium rainfall estimates (Figs. 4g–i) are best represented in Central India and
318 over the Deccan Plateau by TRMM and IMERG. Both show similar statistics over the
319 Western Ghats and basins in North-Eastern and Eastern coast of India. TRMM slightly
320 outperforms IMERG in the North-Western basin of Rajasthan, a trend also found in the low
321 rainfall regime. IMERG doesn't capture the medium rainfall trends over the Upper Indus
322 basin (in Northern India). In general, TRMM-R medium rainfall estimates are best correlated
323 in the semi-arid region of Rajasthan (North-Western basins) and in Central India. There is not
324 much variability in the correlation of medium rainfall trends of TRMM-R, with correlation
325 coefficient mostly around 0.5 for entire India, except for the high elevation Upper Indus
326 basin.

327 The high rainfall estimates (Figs. 4j–k) show highest correlation in the Deccan
328 Plateau belt, higher elevation basins in Northern India, the Western Ghats and the East coast
329 basins (except for the Southern-most basin) for TRMM and IMERG. High rainfall estimates
330 of TRMM are better correlated than IMERG in the North-Eastern basins of Brahmaputra and
331 Barak and the North-Western basins of Rajasthan. Both show similar correlation over the
332 high elevation basins in the North and over the Western Ghats. IMERG outperforms TRMM
333 in the rain-shadow area of the Western Ghats and in the South-Eastern basins of Pennar and
334 Cauvery. Retrospective maps of TRMM-R (Fig. 4j) suggest that high rainfall is adequately
335 captured in the Indo-Gangetic plain, Western Ghats, North-Western basins of Rajasthan,
336 South-Eastern basins of Pennar and Cauvery and the Eastern coast basins of Central India.
337 However, TRMM gives very low correlation values for the rain-shadow belt of the Western
338 Ghats, suggesting that it doesn't capture the steep orographic gradient. The high rainfall
339 estimates of TRMM-R give modest correlation in the North-Eastern basins, high elevation
340 basins in Northern India and the West most basins of the South (Varrar and Periyar).



341 3.3 Basin-wise bias

342 Basin-wise bias was computed for retrospective analysis of TRMM-R and to compare
343 TRMM and IMERG rainfall estimates for the year 2014. Although, IMERG tends to give
344 slightly better correlation on a basin-wise scale (Fig. 3a), Fig. 5a suggests that it also
345 enhances the bias in the product. The bias plot for the low rainfall regime (Fig. 5b) suggests
346 that TRMM is more negatively biased than IMERG for 75 out of 86 basins. Negative bias
347 indicates overestimation, which is a known problem with TRMM as its sensors cannot detect
348 very low rainfall magnitudes (<0.5 mm/hour) (Hou et al., 2014). If it detects a low intensity
349 storm, it is most likely to overestimate it which can be clearly seen in Fig. 5b. IMERG tends
350 to give a better estimate of low rainfall magnitudes with smaller negative biases for 75 out of
351 86 basins, due to the sensor improvements in the GPM mission (Huffman et al., 2014). For
352 the medium rainfall magnitudes, IMERG slightly increased the bias in the majority of basins
353 (63 out of 86). In TRMM, there were 18 basins which showed positive bias which was
354 increased to 38 in IMERG. However, this is not to be misunderstood as a decay in skill as in
355 TRMM there were 28 basins which were relatively unbiased ($-10\% \leq \text{bias} \leq 10\%$) which
356 was increased to 37 in IMERG. IMERG tends to increase the variability of bias in the high
357 rainfall regime (Fig. 5d). For the high rainfall estimates, TRMM has 57 basins whose bias lies
358 between -20% to $+20\%$ which is decreased to 52 in IMERG. In TRMM, 57 basins showed
359 positive bias (implying underprediction) which was reduced to 48 basins in IMERG. This
360 suggests a reduction in systematic underprediction, although with greater variability in bias in
361 IMERG for the high rainfall regime.

362 The spatial maps for the overall rainfall time series (Figs. 6a-c) suggests similar bias
363 patterns in TRMM and IMERG with spatial coherent trends throughout most of India.
364 IMERG gives slightly lower bias over the high elevation basins of North India (Upper Indus
365 basin) and slightly higher bias over the North Eastern basins (of Brahmaputra and Barak) and
366 the West flowing rivers of Kutch on the Western coast in the state of Gujarat. IMERG gives a
367 large negative bias (overprediction) over Upper and Middle Godavari basin (in Deccan
368 Plateau belt) which suggests that the sharp topographic gradient is not well captured.
369 Retrospective maps of TRMM-R suggest an underestimation over high elevation basins in
370 Northern India (Indus, Jhelum and Chenab basins). However, TRMM captures the heavy
371 precipitation on the Western Ghats well with very low biases.



372 The low rainfall spatial maps (Figs. 6d–f) show the large overprediction (negative
373 bias) by TRMM (1998–2013 and 2014) which is improved in IMERG. The improvement is
374 most prominent in the North Eastern basins (of Brahmaputra and Barak), Central India
375 (Mahi, Chambal and the Indo-Gangetic plain), rain-shadow area of the Western Ghats and the
376 South-Eastern coast. IMERG shows gross overprediction over Luni basin (near the Western
377 coast of Rajasthan). Retrospective TRMM-R maps for low rainfall regime (Fig. 6d) show that
378 the low rainfall was best captured in high rainfall areas of the Western Ghats, the Indo-
379 Gangetic plain and the Eastern coastal basins, which is not very surprising as TRMM doesn't
380 detect low rainfall magnitudes very well, thus suffering from overprediction in arid and semi-
381 arid basins. Improvement in the low rainfall sensors in IMERG has improved low rainfall
382 estimates, but it still suffers from gross overprediction in semi-arid areas (as evident in the
383 semi-arid basins in North-West India (Fig. 6f).

384 The medium rainfall spatial maps (Figs. 6g–i) suggest very similar spatial bias pattern
385 in TRMM and IMERG, with low biases in most of the basins. Both TRMM and IMERG
386 suffer from underprediction (positive bias) in the high elevation Northern basins (of Indus
387 and Jhelum), although IMERG seem to be less biased than TRMM. Both show similar trends
388 in the Western Ghats, with very low bias. However, both the products show large negative
389 bias (overprediction) in the Middle Godavari basin, unable to capture the sharp topographic
390 gradient in the region. IMERG slightly overpredicts rainfall in the North Eastern basins (of
391 Brahmaputra and Barak). The retrospective TRMM maps for medium rainfall (Fig. 6g) show
392 almost constant bias (almost unbiased) over entire India, except over the Western Ghats
393 (slightly positive bias (slight underprediction)) and high elevation Northern basins of Indus
394 and Jhelum (positive bias (strong underprediction)).

395 The high rainfall spatial maps (Figs. 6j–l) suggest similar spatial pattern in TRMM
396 and IMERG, with slight negative bias over majority of the basins. The high rainfall in the
397 Western Ghats is well represented in TRMM and IMERG, with overprediction in the leeward
398 side of the Western Ghats, suggesting that IMERG is unable to capture the sharp topographic
399 gradients. IMERG shows slightly greater bias (implying greater underprediction) in the high
400 rainfall areas of the North Eastern basins. IMERG gives a better estimate (still underpredicts)
401 in the high elevation basins in Northern India. Both IMERG and TRMM give similar bias
402 pattern in the Indo-Gangetic plain and the semi-arid areas of the North-West. The
403 retrospective TRMM-R map for high rainfall (Fig. 6j) suggests that TRMM slightly
404 overpredicts high rainfall in majority of India (Indo-Gangetic plain, Deccan Plateau, rain-



405 shadow area of the Western Ghats). However, it suffers from gross underestimation in the
406 high elevation basins of Northern India (Indus, Jhelum and Chenab). It is clearly observed
407 that the high elevation basins are an outlier in most of the analysis, a systematic dependence
408 of bias with elevation may be an underlying trend which is further explored in section *e*.

409 3.4 Threshold statistics

410 Basin-wise POD and FAR was computed for retrospective analysis of TRMM-R and
411 for the comparison of TRMM with IMERG (Figs. 7 and 8). Four rainfall thresholds were
412 chosen, representative of different rainfall regimes (low threshold: 25 percentile, medium
413 threshold: 50 percentile, high threshold: 75 percentile and very high threshold: 95 percentile).
414 Increasing rainfall threshold leads to deteriorating trends in POD and FAR across majority of
415 the basins, with decreasing POD and increasing FAR.

416 For the low rainfall threshold, IMERG gives higher POD than TRMM for 62 basins,
417 with the major improvement in the Western region of Gujarat (Luni, Bhadar and Setrunji
418 basins) (Figs. 7b,c). There is less spatial variability in POD for both TRMM and IMERG at
419 low rainfall threshold with POD above 0.9 for 75 basins for IMERG and 63 basins for
420 TRMM. The average POD (low rainfall threshold) across basins is 0.95 for IMERG and 0.91
421 for TRMM. For the medium rainfall threshold, IMERG outperforms TRMM in 39 basins
422 with TRMM giving a higher POD in 37 basins; both the products give similar POD in 10
423 basins. The average POD (medium rainfall threshold) across basins is 0.87 for both IMERG
424 and TRMM. Notably, IMERG gives lower POD (medium rainfall threshold) in 2 (Barak and
425 Brahmaputra lower sub-basin) out of the 3 North-Eastern basins, and higher POD (medium
426 rainfall threshold) in the semi-arid basins of Rajasthan and Gujarat (Luni, Bhadar and
427 Setrunji basins) (Figs. 7e,f). For the high rainfall threshold, TRMM outperforms IMERG in
428 45 basins with IMERG giving a higher POD in 32 basins, both the products give similar POD
429 in 9 basins. The average POD (high rainfall threshold) across basins is 0.76 for IMERG and
430 0.77 for TRMM. There is notable fall in performance in all the 3 North-Western basins.
431 IMERG gives slightly higher POD (high rainfall threshold) in the high elevation Northern
432 basins (Upper Indus and Jhelum basins) (Figs. 7h,i). For the very high rainfall threshold,
433 IMERG outperforms TRMM in 44 basins with TRMM giving a higher POD in 27 basins;
434 both the products give similar POD in 15 basins. The average POD (very high rainfall
435 threshold) across basins is 0.72 for IMERG and 0.7 for TRMM. At very high rainfall
436 threshold, it's clear that POD of IMERG is worse for all the 3 North-Eastern basins and over



437 the semi-arid basins of Rajasthan and Gujarat (Figs. 7k,i). There is slight improvement in
438 POD values for the high elevation Northern basins (Chenab, Ravi, Beas and Satulaj basins).

439 At low rainfall threshold, TRMM gives higher FAR than IMERG in 42 basins with
440 IMERG giving a higher FAR in 40 basins; both the products give similar FAR in 4 basins.
441 The average FAR (low rainfall threshold) across basins is 0.24 for TRMM and 0.22 for
442 IMERG. For the medium rainfall threshold, IMERG outperforms TRMM (with lower FAR)
443 in 53 basins with TRMM giving lower FAR in 26 basins; both the products give similar FAR
444 in 7 basins. The average FAR (medium rainfall threshold) across basins is 0.22 for TRMM
445 and 0.19 for IMERG. Notably, IMERG outperforms TRMM at low and medium rainfall
446 thresholds giving lower FAR in the Western basins of Gujarat (Luni and Setrunji basins)
447 (Figs. 8b,c,e,f). For the high rainfall threshold, IMERG outperforms TRMM in 67 basins
448 (lower FAR) with TRMM giving a lower FAR in 15 basins; both the products give similar
449 FAR in 4 basins. The average FAR (high rainfall threshold) across basins is 0.18 for IMERG
450 and 0.22 for TRMM. Slightly reduced FAR are seen in Central India (Yamuna and Chambal
451 basins) and the North-Eastern basins (Brahmaputra basin) in IMERG at high rainfall
452 threshold (Figs. 8h,i). For the very high rainfall threshold, IMERG outperforms TRMM in 64
453 basins (lower FAR) with TRMM giving a lower FAR in 17 basins; both the products give
454 similar FAR in 5 basins. The average FAR (very high rainfall threshold) across basins is 0.33
455 for IMERG and 0.41 for TRMM. There are notably fewer false alarms in IMERG estimates
456 over the Northern, North-Eastern basins and the Western Ghats at very high thresholds. Both
457 products give similar FAR (very high threshold) along the Eastern coast and Deccan Plateau
458 basins.

459 POD for TRMM-R suggests decreasing POD and increasing FAR with increasing
460 rainfall threshold (Figs. 7a,d,g,j, Figs. 8a,d,g,j). The average POD across basins is 0.89, 0.85,
461 0.77 and 0.66 for low, medium, high and very high rainfall thresholds, respectively. The
462 respective FAR values are 0.26, 0.22, 0.21 and 0.43. At high and very high threshold, POD
463 drops significantly over the high elevation Northern basins and high rainfall North-Eastern
464 basins and the Western Ghats) (Figs. 7g,j). High FAR is recorded in the basins in Gujarat
465 (Luni and Setrunji) and Central India (Bhadar and Chambal) at low and medium rainfall
466 threshold (Figs. 8a,d) suggesting TRMM creates a lot of false alarms at low and medium
467 rainfall magnitudes. There is a sharp contrast between FAR at high and very high thresholds,
468 with low FAR at high rainfall threshold (75 percentile) and high FAR at very high threshold
469 (95 percentile) (Figs. 8g,j). This suggests that TRMM-R creates a lot of false alarms at very



470 high rainfall thresholds, especially in the North-Eastern, Northern and extreme Southern
471 basins (Fig 8j).

472 **3.5 Systematic error in satellite estimates as a function of annual rainfall and mean** 473 **elevation**

474 The satellite precipitation estimates were evaluated against a climatologic parameter
475 (long term annual rainfall of basin) and a topographic parameter (basin mean elevation). Fig.
476 9 describes the relationship between mean annual precipitation and mean elevation by
477 considering the point values for 86 basins. It was found that there is no systematic
478 dependence between the climatologic and topographic parameter ($R = 0.07$) and they can be
479 considered as independent (implying minimal interference).

480 TRMM-R rainfall estimates exhibited strong systematic dependence of bias and
481 correlation with basin wise mean rainfall at low and medium rainfall estimates (Figs. 10 and
482 11). At low rainfall regime, TRMM-R estimates for basins experiencing low annual rainfall
483 were found to be strongly negatively biased (Fig. 10b), implying significant overprediction.
484 The bias values improved drastically for basins experiencing higher annual rainfall. This is
485 also reflected in the correlation plots (Fig. 11b), where a positive correlation between basin-
486 wise correlation and annual rainfall ($R = 0.3$) implies improved estimates of low rainfall at
487 basins which experience high annual rainfall. At the medium rainfall regime, TRMM-R
488 estimates showed higher bias (implying underprediction) and lower correlation (reduced
489 skill) in basins receiving higher annual rainfall, with a sharp drop in correlation for heavy
490 rainfall basins (Figs. 10c and 11c). At high rainfall regime, the systematic bias was reduced,
491 both in terms of percent bias and correlation, implying that there is no significant difference
492 in TRMM-R estimates of high rainfall, in basins receiving low/high annual rainfall.

493 For the year 2014, both IMERG and TRMM showed increasing bias as a function of
494 increasing annual rainfall for all the rainfall regimes (Fig. 12), with the systematic
495 dependence strongly reduced in IMERG estimates for the medium rainfall regime. For the
496 low rainfall regime, bias and correlation values improve for basins receiving higher rainfall
497 (Figs. 12b and 13b). TRMM and IMERG showed similar systematic dependence on annual
498 rainfall at low rainfall regime, with correlation values between basin wise correlation and
499 annual rainfall equal to 0.38 and 0.39 for TRMM and IMERG, respectively. For the medium
500 rainfall regime, both IMERG and TRMM showed increasing bias with increasing annual
501 basin-wise rainfall (Fig. 12c). However, there was a strong reduction in the systematic bias



502 component in IMERG, with correlation between basin-wise bias and rainfall decreasing from
503 0.43 (for TRMM) to 0.3 (for IMERG). At medium rainfall, a substantial skill was lost in
504 terms of decreasing correlation for basins receiving high rainfall (Fig. 13c). This systematic
505 dependence wasn't reduced in IMERG estimates, with correlation values between basin-wise
506 correlation and rainfall as -0.45 for TRMM and -0.44 for IMERG. At high rainfall regime,
507 bias was higher for basins which received more rainfall, implying greater underprediction in
508 basins with heavy rainfall magnitude (Fig. 12d). This systematic bias wasn't reduced in
509 IMERG estimates. No systematic dependence was found in the correlation of
510 IMERG/TRMM estimates with basin-wise rainfall (Fig. 13d).

511 TRMM-R rainfall estimates exhibited very strong dependence on mean basin
512 elevation, with decreasing skill (higher bias and lower correlation) in basins with high mean
513 elevation (Figs. 14 and 15). For the low rainfall regime, a correlation coefficient (between
514 basin-wise bias and elevation) of (-0.08) (Fig. 14b) may suggest that there is no systematic
515 dependence between elevation and bias. For medium and high rainfall regimes (Figs. 14c, d),
516 bias values increase drastically for high elevation basins (especially for basins with mean
517 elevation > 2000 m), implying underprediction at higher elevations. The corresponding
518 correlation values (Figs. 15c, d) also suggest reduced skill at higher elevation basins.

519 For the year 2014, except at low rainfall magnitude, bias increases with mean basin
520 elevation for TRMM and IMERG rainfall estimates (Fig. 16). This systematic dependence of
521 bias on basin elevation is improved in IMERG estimates, with the correlation between basin-
522 wise bias and elevation reducing from 0.43 to 0.32 for medium rainfall regime (Fig. 16c) and
523 from 0.31 to 0.08 for high rainfall regime (Fig. 16d). It's interesting to note that the same is
524 not seen for the correlation plots (Fig. 17). For the low rainfall regime (Fig. 17b), IMERG
525 estimates exhibit stronger systematic relationship between basin-wise correlation and
526 elevation, with strongly decreasing correlation with elevation than TRMM. At medium
527 rainfall intensity (Fig. 17c), both TRMM and IMERG show decreasing skill with increasing
528 elevation. This systematic dependence is again stronger in IMERG than TRMM, as reflected
529 in the higher negative correlation between basin-wise correlation and elevation in medium
530 rainfall IMERG estimates (Fig. 17c). For the high rainfall intensity (Fig. 17d), both IMERG
531 and TRMM do not show any systematic dependence of skill with elevation.

532 3.6 Rainfall-runoff modeling



533 Rainfall-runoff modeling was carried out over HiraKud catchment of Mahanadi River
534 basin with the calibration and validation periods as 2000-2011 and 2012-2014, respectively.
535 VIC was first calibrated with IMD gridded precipitation and then with TRMM3B42 V7. The
536 two calibrated models were then forced with TRMM and IMERG precipitation forcing for
537 the year 2014 (April – December). Table 5 shows the model performance.

538 VIC was successfully calibrated using IMD (NSE = 0.83 for calibration and 0.86 for
539 validation) and TRMM (NSE = 0.72 for calibration and 0.73 for validation). The IMD
540 calibrated model showed better simulations compared to the TRMM calibrated model, with
541 higher NSE, coefficient of determination and lower bias and RMSE. TRMM calibrated model
542 showed slight overprediction (negative bias) (Table 5).

543 The IMERG simulations with IMD and TRMM calibrated models were slightly
544 inferior in comparison with TRMM simulations for 2014 (Table 5, Fig. 18). The IMERG
545 simulations with TRMM calibrated model reported higher NSE and coefficient of
546 determination, with lower bias and RMSE, which might be due to the fact that TRMM and
547 IMERG are both satellite products and exhibit similar spatio-temporal trends. The high
548 negative bias in IMERG simulations (with IMD and TRM calibrated models) showed
549 significant overprediction compared to TRMM.

550 Both TRMM and IMERG underestimated the magnitude of the two major peaks (flow
551 > 15000 m³/s) in 2014. However, the phase was well captured by both IMERG and TRMM.
552 Apart from the two major peaks, IMERG overestimated flow for the majority of the time in
553 both IMD and TRMM calibrated VIC model (hence the negative bias value), and thus was
554 inferior in performance to TRMM. This suggests that the use of an appropriate post-
555 processor (in form of real-time error updation) could tremendously benefit the flow
556 simulations, which might be an interesting study for the future.

557 **4 Conclusions**

558 TRMM 3B42 and IMERG precipitation estimates were comprehensively evaluated over
559 86 basins in India. TRMM 3B42 was analysed for two distinct time periods, the retrospective
560 analysis was carried out from 1998-2013 and the current estimates were compared with
561 IMERG for the year 2014 (March 12th 2014 – December 31st 2014). The systematic biases in
562 both the estimates were explored with respect to a climatologic parameter (basin mean annual
563 rainfall) and a topographic parameter (basin mean elevation). Finally, TRMM and IMERG



564 were hydrologically evaluated by carrying out rainfall-runoff modeling over Hirakud
565 catchment of Mahanadi River basin, a flood prone basin in Eastern India. The results of the
566 study are summarized as:

- 567 1. IMERG rainfall estimates were found to be better than TRMM at all rainfall intensities.
568 IMERG outperformed TRMM in 60, 52, 52 and 55 out of 86 basins for overall, low,
569 medium and high rainfall regimes.
- 570 2. IMERG gave better estimates of low rainfall magnitudes with smaller negative biases in
571 75 out of the 86 basins analysed, which suggests that the sensor improvement in IMERG
572 satellite translated into better low rainfall estimation. IMERG captured the low rainfall
573 magnitudes better over the Indo-Gangetic plain, North Eastern basins of Brahmaputra and
574 Barak, Central India (Mahi, Chambal and the Indo-Gangetic plain) and the rain shadow
575 area of the Western Ghats. However, for the semi-arid North Western basins, TRMM low
576 rainfall estimates outperformed IMERG.
- 577 3. The high rainfall estimates of IMERG outperformed TRMM in the rain-shadow area of
578 the Western Ghats, the high elevation basins of the North and the South-Eastern basins of
579 Pennar and Cauvery. However, TRMM did a better job in the North-Eastern basins of
580 Brahmaputra and Barak and the North-Western basins of Rajasthan. Interestingly,
581 IMERG reduced the systematic underprediction over TRMM although with greater
582 variability in bias at high rainfall intensity.
- 583 4. Increasing rainfall thresholds lead to deteriorating trends in POD and FAR across
584 majority of basins, with decreasing POD and increasing FAR.
- 585 5. The skill of TRMM-R medium rainfall estimates (in terms of Pbias and correlation) was
586 found to exhibit strong systematic dependence on annual rainfall (climatologic
587 parameter), with higher bias and lower correlation in basins which received higher annual
588 rainfall. This systematic dependence was reduced significantly in IMERG estimates.
589 However, no such improvement was found at low and high rainfall intensities.
- 590 6. A very strong deteriorating skill (increasing bias and decreasing correlation) was found in
591 TRMM-R rainfall estimates at all intensities in the high elevation basins. This systematic
592 dependence was strongly reduced in IMERG estimates at all rainfall intensities,
593 suggesting IMERG captures the rainfall trends better with respect to topography.
- 594 7. Rainfall runoff modeling using VIC model over Hirakud catchment of the Mahanadi
595 River basin gave better results with TRMM as input forcing, rather than IMERG. Both
596 TRMM and IMERG captured the phase of the peak flows, however both underreported



597 the magnitudes. Low flows were grossly over predicted by IMERG, which led to overall
598 poor performance with IMERG. As longer timeseries of IMERG is available, it may help
599 in model performance as IMERG can be used to directly calibrate the model, hence
600 capturing the fine details in the product.

601 In essence, IMERG gives reasonable improvement in rainfall estimates across majority of
602 the Indian basins. However, the improvement was not found to be ground breaking, rather
603 incremental, suggesting that the GPM mission is a worthy successor of the widely acclaimed
604 TRMM mission. The most notable improvement in IMERG is the reduction in systematic
605 error dependence on topography (basin mean elevation), which suggests improvements in the
606 assimilation of satellite observations. The improved sensitivity of Ku and Ka bands in GPM
607 satellite resulted in improvement in detection of low rainfall magnitudes. The expected
608 improvement in IMERG in snow detection could not be verified in this study as India is
609 mostly a tropical country which receives very less snow. The constant overestimation of low
610 flow magnitudes in the rainfall-runoff exercise suggest that IMERG may benefit from a post
611 forecast data assimilation scheme, which is a worthy topic for further research.



612 **References**

- 613 Akhtar, M. K., Corzo, G. A., van Andel, S. J. and Jonoski, A.: River flow forecasting with
614 artificial neural networks using satellite observed precipitation pre-processed with flow
615 length and travel time information: case study of the Ganges river basin, *Hydrol. Earth Syst.*
616 *Sci.*, 13(9), 1607–1618, doi:10.5194/hess-13-1607-2009, 2009.
- 617 Artan, G., Gadain, H., Smith, J. L., Asante, K., Bandaragoda, C. J. and Verdin, J. P.:
618 Adequacy of satellite derived rainfall data for stream flow modeling, *Nat. Hazards*, 43, 167–
619 185, doi:10.1007/s11069-007-9121-6, 2007.
- 620 Bajracharya, S. R., Shrestha, M. S. and Shrestha, A. B.: Assessment of high-resolution
621 satellite rainfall estimation products in a streamflow model for flood prediction in the
622 Bagmati basin, Nepal, *J. Flood Risk Manag.*, 1–12, doi:10.1111/jfr3.12133, 2014.
- 623 Collischonn, B., Collischonn, W. and Tucci, C. E. M.: Daily hydrological modeling in the
624 Amazon basin using TRMM rainfall estimates, *J. Hydrol.*, 360, 207–216,
625 doi:10.1016/j.jhydrol.2008.07.032, 2008.
- 626 Duband, D., Obled, C. and Rodriguez, J. Y.: Unit hydrograph revisited: an alternate iterative
627 approach to UH and effective precipitation identification, *J. Hydrol.*, 150(1), 115–149,
628 doi:10.1016/0022-1694(93)90158-6, 1993.
- 629 Gao, Y. C. and Liu, M. F.: Evaluation of high-resolution satellite precipitation products using
630 rain gauge observations over the Tibetan Plateau, *Hydrol. Earth Syst. Sci.*, 17(2), 837–849,
631 doi:10.5194/hess-17-837-2013, 2013.
- 632 Hamlet, A. F. and Lettenmaier, D. P.: Columbia River Streamflow Forecasting Based on
633 ENSO and PDO Climate Signals, *J. Water Resour. Plan. Manag.*, 125(6), 333–341,
634 doi:10.1061/(ASCE)0733-9496(1999)125:6(333), 1999.
- 635 Hou, A. Y., Kakar, R. K., Neeck, S., Azarbarzin, A. A., Kummerow, C. D., Kojima, M., Oki,
636 R., Nakamura, K. and Iguchi, T.: The Global Precipitation Measurement Mission, *Bull. Am.*
637 *Meteorol. Soc.*, 95(5), 701–722, doi:10.1175/BAMS-D-13-00164.1, 2014.
- 638 Huffman, G. J., Bolvin, D. T., Nelkin, E. J., Wolff, D. B., Adler, R. F., Gu, G., Hong, Y.,
639 Bowman, K. P. and Stocker, E. F.: The TRMM Multisatellite Precipitation Analysis (TMPA):
640 Quasi-Global, Multiyear, Combined-Sensor Precipitation Estimates at Fine Scales, *J.*



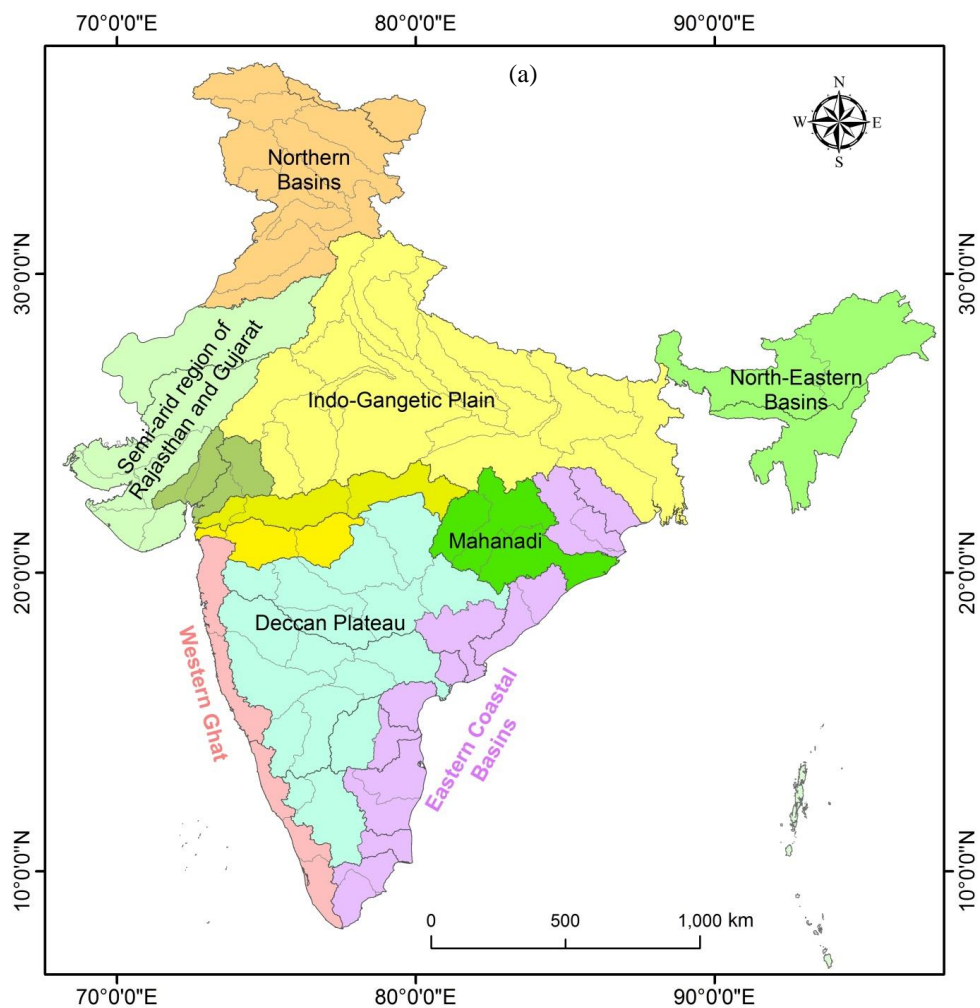
- 641 Hydrometeorol., 8(1), 38–55, doi:10.1175/JHM560.1, 2007.
- 642 Huffman, G. J., Bolvin, D. T. and Nelkin, E. J.: Integrated Multi-satellitE Retrievals for GPM
643 (IMERG) Technical Documentation, 2014.
- 644 India, G. of: Watershed Atlas of India. [online] Available from: [http://india-](http://india-wris.nrsc.gov.in/Publications/WatershedSubbasinAtlas/Watershed Atlas of India.pdf)
645 [wris.nrsc.gov.in/Publications/WatershedSubbasinAtlas/Watershed Atlas of India.pdf](http://india-wris.nrsc.gov.in/Publications/WatershedSubbasinAtlas/Watershed Atlas of India.pdf), 2014.
- 646 Jena, P. P., Chatterjee, C., Pradhan, G. and Mishra, A.: Are recent frequent high floods in
647 Mahanadi basin in eastern India due to increase in extreme rainfalls?, J. Hydrol., 517, 847–
648 862, doi:10.1016/j.jhydrol.2014.06.021, 2014.
- 649 Kneis, D., Chatterjee, C. and Singh, R.: Evaluation of TRMM rainfall estimates over a large
650 Indian river basin (Mahanadi), Hydrol. Earth Syst. Sci., 18(7), 2493–2502 [online] Available
651 from: <http://www.hydrol-earth-syst-sci-discuss.net/11/1169/2014/hessd-11-1169-2014.pdf>
652 (Accessed 20 October 2014), 2014.
- 653 Liang, X., Lettenmaier, D. P., Wood, E. F. and Burges, S. J.: A simple hydrologically based
654 model of land surface water and energy fluxes for general circulation models, J. Geophys.
655 Res., 99(D7), 14415, doi:10.1029/94JD00483, 1994.
- 656 Liang, X., Wood, E. F. and Lettenmaier, D. P.: Surface soil moisture parameterization of the
657 VIC-2L model: Evaluation and modification, Glob. Planet. Change, 13, 195–206,
658 doi:10.1016/0921-8181(95)00046-1, 1996.
- 659 Liu, Z.: Comparison of Integrated Multi-satellitE Retrievals for GPM (IMERG) and TRMM
660 Multi-satellite Precipitation Analysis (TMPA) Monthly Precipitation Products: Initial
661 Results, J. Hydrometeorol., 17, 777–790, doi:10.1175/JHM-D-15-0068.1, 2016.
- 662 Lohmann, D., Nolte-Holube, R. and Raschke, E.: A large-scale horizontal routing model to
663 be coupled to land surface parametrization schemes, Tellus A, 48(5), 708–721,
664 doi:10.1034/j.1600-0870.1996.t01-3-00009.x, 1996.
- 665 McCuen, R. H.: Assessment of Hydrological and Statistical Significance, J. Hydrol. Eng.,
666 21(4), 02516001, doi:10.1061/(ASCE)HE.1943-5584.0001340, 2016.
- 667 Melsen, L. A., Teuling, A. J., Torfs, P. J. J. F., Uijlenhoet, R., Mizukami, N. and Clark, M.
668 P.: HESS Opinions: The need for process-based evaluation of large-domain hyper-resolution
669 models, Hydrol. Earth Syst. Sci., 20(3), 1069–1079, doi:10.5194/hess-20-1069-2016, 2016.



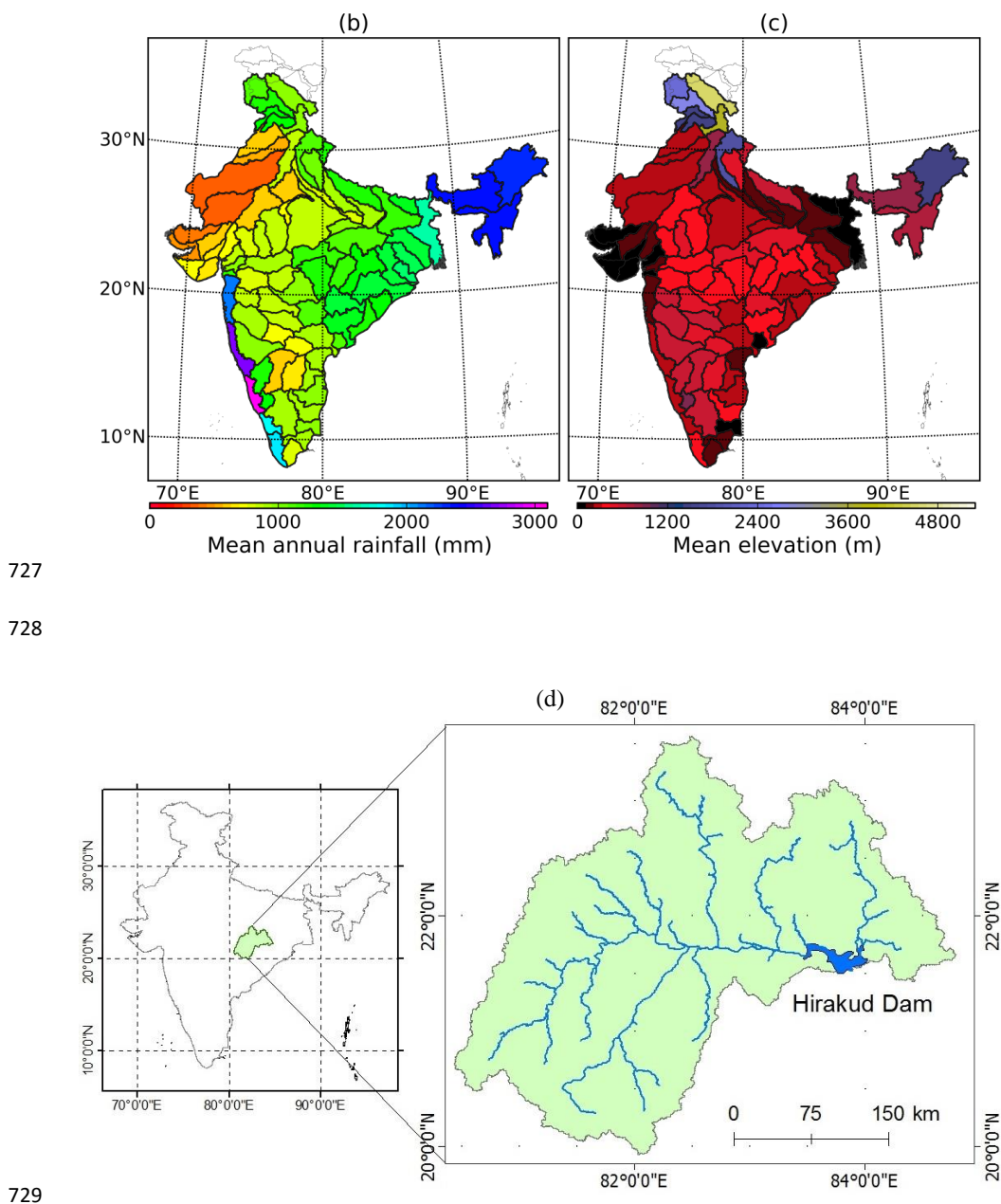
- 670 Mujumdar, P. P.: Share data on water resources, *Nature*, 521(7551), 151–152, 2015.
- 671 Pai, D. S., Sridhar, L., Rajeevan, M., Sreejith, O. P., Satbhai, N. S. and Mukhopadhyay, B.:
672 Development of a new high spatial resolution (0.25× 0.25) long period (1901–2010) daily
673 gridded rainfall data set over India and its comparison with existing data sets over the region.,
674 *Mausam*, 65(1), 1–18, 2014.
- 675 Peng, B., Shi, J., Ni-Meister, W., Zhao, T. and Ji, D.: Evaluation of TRMM Multisatellite
676 Precipitation Analysis (TMPA) Products and Their Potential Hydrological Application at an
677 Arid and Semiarid Basin in China, *IEEE J. Sel. Top. Appl. Earth Obs. Remote Sens.*, 7(9),
678 3915–3930, doi:10.1109/JSTARS.2014.2320756, 2014.
- 679 Prakash, S., Mitra, A. K., Momin, I. M., Gairola, R. M., Pai, D. S., Rajagopal, E. N. and
680 Basu, S.: A review of recent evaluations of TRMM Multisatellite Precipitation Analysis
681 (TMPA) research products against ground-based observations over Indian land and oceanic
682 regions, *MAUSAM*, 66(3), 355–366 [online] Available from:
683 [https://www.researchgate.net/profile/Satya_Prakash/publication/281115874_A_review_of_re](https://www.researchgate.net/profile/Satya_Prakash/publication/281115874_A_review_of_recent_evaluations_of_TRMM_Multisatellite_Precipitation_Analysis_(TMPA)_research_products_against_ground-based_observations_over_Indian_land_and_oceanic_regions/links/55e)
684 [cent_evaluations_of_TRMM_Multisatellite_Precipitation_Analysis_\(TMPA\)_research_pro](https://www.researchgate.net/profile/Satya_Prakash/publication/281115874_A_review_of_recent_evaluations_of_TRMM_Multisatellite_Precipitation_Analysis_(TMPA)_research_products_against_ground-based_observations_over_Indian_land_and_oceanic_regions/links/55e)
685 [ducts_against_ground-based_observations_over_Indian_land_and_oceanic_regions/links/55e](https://www.researchgate.net/profile/Satya_Prakash/publication/281115874_A_review_of_recent_evaluations_of_TRMM_Multisatellite_Precipitation_Analysis_(TMPA)_research_products_against_ground-based_observations_over_Indian_land_and_oceanic_regions/links/55e),
686 2015.
- 687 Prakash, S., Mitra, A. K., AghaKouchak, A., Liu, Z., Norouzi, H. and Pai, D. S.: A
688 preliminary assessment of GPM-based multi-satellite precipitation estimates over a monsoon
689 dominated region, *J. Hydrol.*, doi:10.1016/j.jhydrol.2016.01.029, 2016a.
- 690 Prakash, S., Mitra, A. K., Pai, D. S. and AghaKouchak, A.: From TRMM to GPM: How well
691 can heavy rainfall be detected from space?, *Adv. Water Resour.*, 88, 1–7,
692 doi:10.1016/j.advwatres.2015.11.008, 2016b.
- 693 Shah, H. L. and Mishra, V.: Uncertainty and Bias in Satellite-based Precipitation Estimates
694 over Indian Sub-continental Basins: Implications for Real-time Streamflow Simulation and
695 Flood Prediction, *J. Hydrometeorol.*, 17(2), 615–636, doi:10.1175/JHM-D-15-0115.1, 2015.
- 696 Srivastava, A. K., Rajeevan, M. and Kshirsagar, S. R.: Development of a high resolution
697 daily gridded temperature data set (1969–2005) for the Indian region, *Atmos. Sci. Lett.*, 10(4),
698 249–254, doi:10.1002/asl.232, 2009.
- 699 Tang, G., Ma, Y., Long, D., Zhong, L. and Hong, Y.: Evaluation of GPM Day-1 IMERG and



- 700 TMPA Version-7 legacy products over Mainland China at multiple spatiotemporal scales, J.
701 Hydrol., 533, 152–167, doi:10.1016/j.jhydrol.2015.12.008, 2016a.
- 702 Tang, G., Zeng, Z., Long, D., Guo, X., Yong, B., Zhang, W. and Hong, Y.: Statistical and
703 Hydrological Comparisons between TRMM and GPM Level-3 Products over a Midlatitude
704 Basin: Is Day-1 IMERG a Good Successor for TMPA 3B42V7?, J. Hydrometeorol., 17(1),
705 121–137, doi:10.1175/JHM-D-15-0059.1, 2016b.
- 706 Tawde, S. A. and Singh, C.: Investigation of orographic features influencing spatial
707 distribution of rainfall over the Western Ghats of India using satellite data, Int. J. Climatol.,
708 35(9), 2280–2293, doi:10.1002/joc.4146, 2015.
- 709 Tong, K., Su, F., Yang, D. and Hao, Z.: Evaluation of satellite precipitation retrievals and
710 their potential utilities in hydrologic modeling over the Tibetan Plateau, J. Hydrol., 519, 423–
711 437, doi:10.1016/j.jhydrol.2014.07.044, 2014.
- 712 Wu, H., Adler, R. F., Hong, Y., Tian, Y. and Policelli, F.: Evaluation of Global Flood
713 Detection Using Satellite-Based Rainfall and a Hydrologic Model, J. Hydrometeorol., 13(4),
714 1268–1284, doi:10.1175/JHM-D-11-087.1, 2012.
- 715 Wu, X., Xiang, X., Li, L. and Wang, C.: Water level updating model for flow calculation of
716 river networks, Water Sci. Eng., 7(1), 60–69, doi:10.3882/j.issn.1674-2370.2014.01.007,
717 2014.
- 718 Yong, B., Hong, Y., Ren, L.-L., Gourley, J. J., Huffman, G. J., Chen, X., Wang, W. and
719 Khan, S. I.: Assessment of evolving TRMM-based multisatellite real-time precipitation
720 estimation methods and their impacts on hydrologic prediction in a high latitude basin, J.
721 Geophys. Res., 117(D9), doi:10.1029/2011JD017069, 2012.
- 722 Zhu, Q., Xuan, W., Liu, L. and Xu, Y.: Evaluation and hydrological application of
723 precipitation estimates derived from PERSIANN CDR, TRMM 3B42V7 and NCEP CFSR
724 over humid regions in China, Hydrol. Process., doi:10.1002/hyp.10846, 2016.
- 725



726

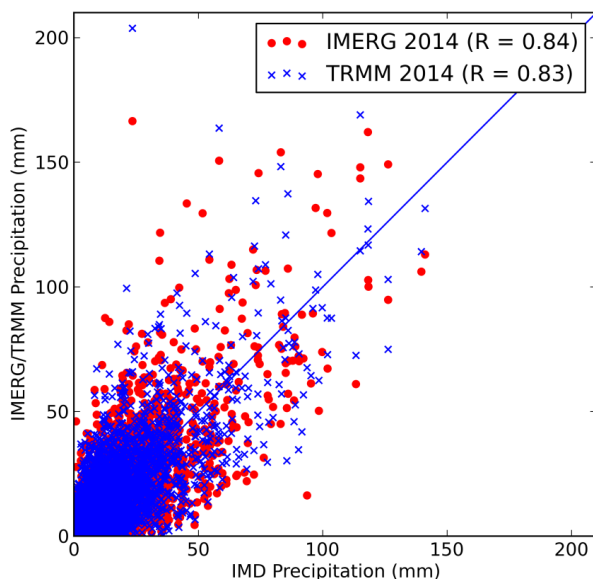


727

728

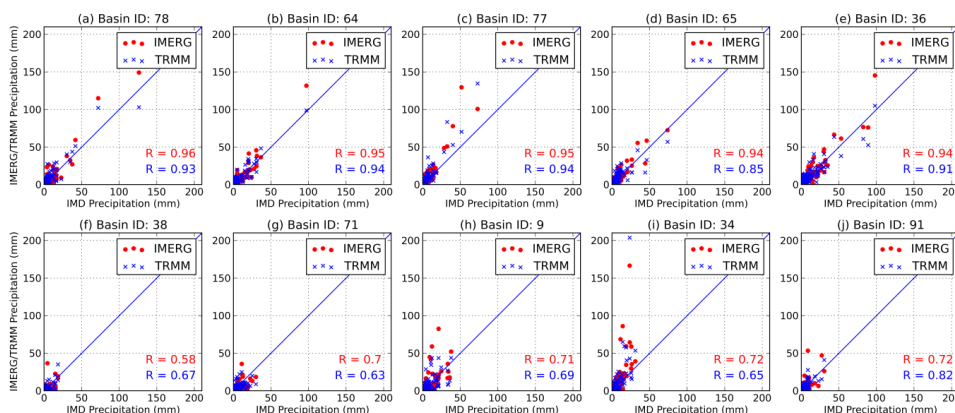
729

730 **Figure 1.**(a) Map of the major basins in India, spatial distribution of (b) long term average
731 annual rainfall (calculated from IMD gridded rainfall dataset from years 1980-2010), (c)
732 average elevation above mean sea level (calculated using SRTM DEM) over 86 major basins
733 in India and (d) map of Hirkud dam catchment of the Mahanadi River basin in Eastern India.



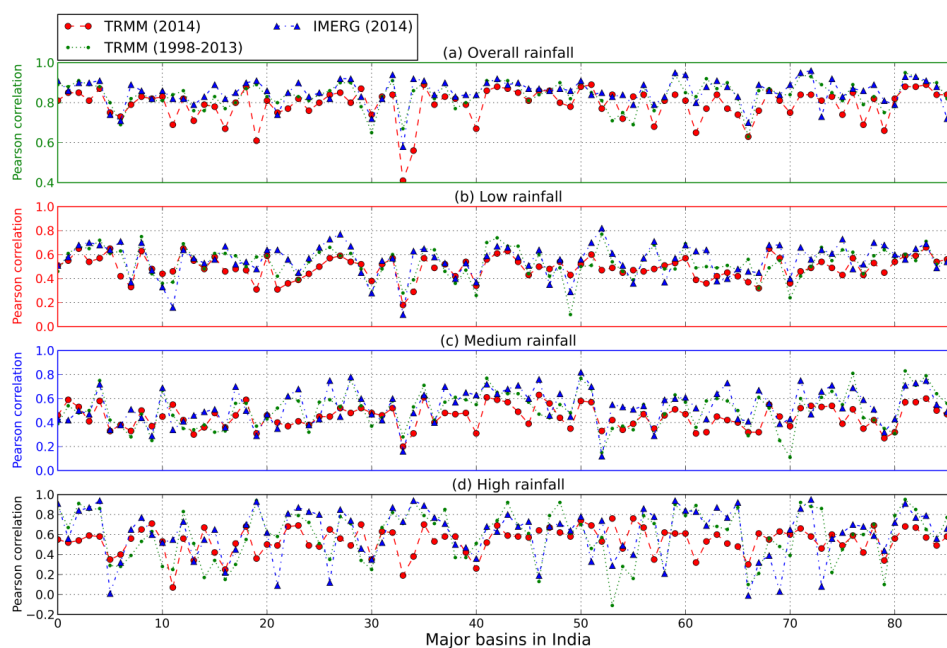
734

735 **Figure 2.1** Scatterplot of satellite precipitation products (TRMM and IMERG) vs observed
 736 rainfall (IMD) computed over 86 major basins in India (from March 12, 2014 to December
 737 31, 2014).



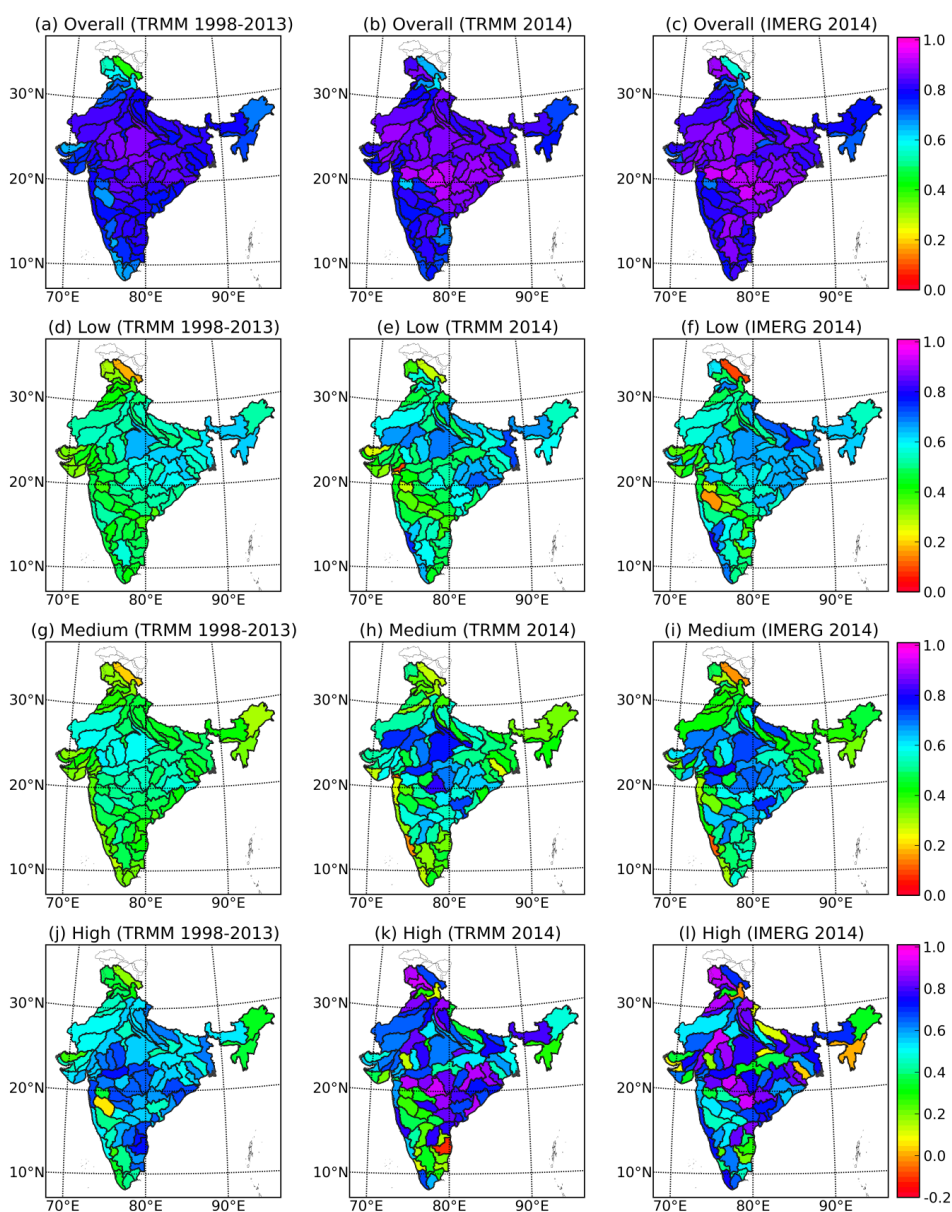
738

739 **Figure 2.2.** Scatterplot of satellite precipitation products (TRMM and IMERG) vs observed
 740 rainfall (IMD) for (a) – (e) five best basins in terms of correlation of IMERG with IMD
 741 (arranged in descending order) and (f) – (j) five worse basins in terms of correlation of
 742 IMERG with IMD (arranged in ascending order) (from March 12, 2014 to December 31,
 743 2014).



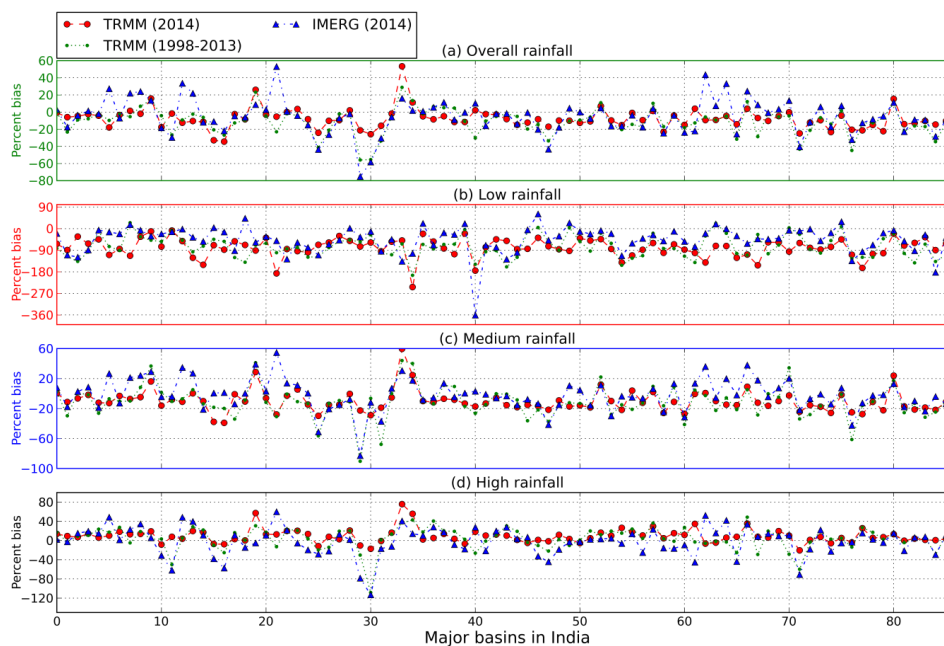
744

745 **Figure 3.** Correlation of TRMM (1998-2013), TRMM (2014) and IMERG (2014) over 86
746 major basins in India for (a) overall time series and over (b) low, (c) medium and (d) high
747 rainfall regime.



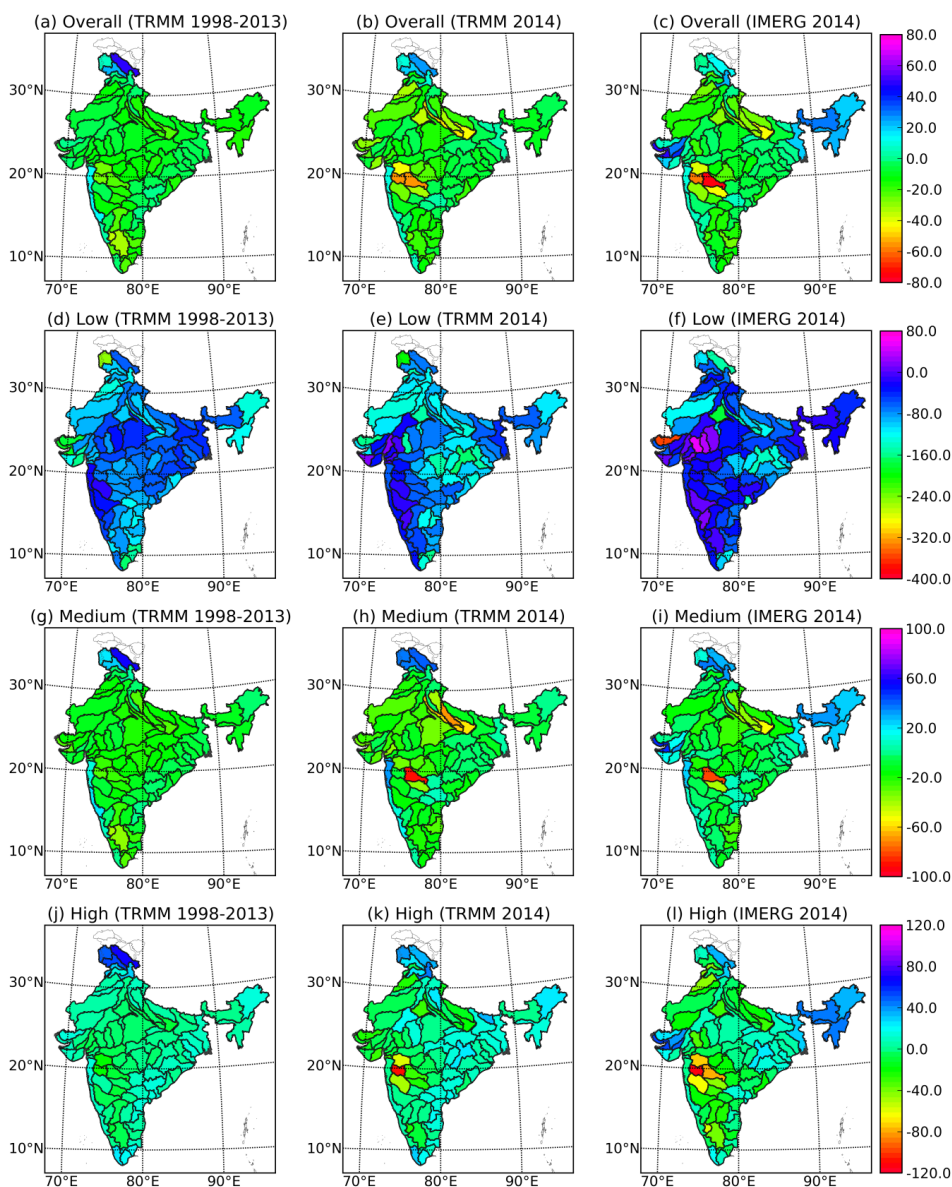
748

749 **Figure 4.** Spatial representation of correlation of TRMM (1998-2013), TRMM (2014) and
750 IMERG (2014) over 86 major basins in India for (a) – (c) overall time series, (d) – (f) low,
751 (g) – (i) medium and (j) – (l) high rainfall regime.



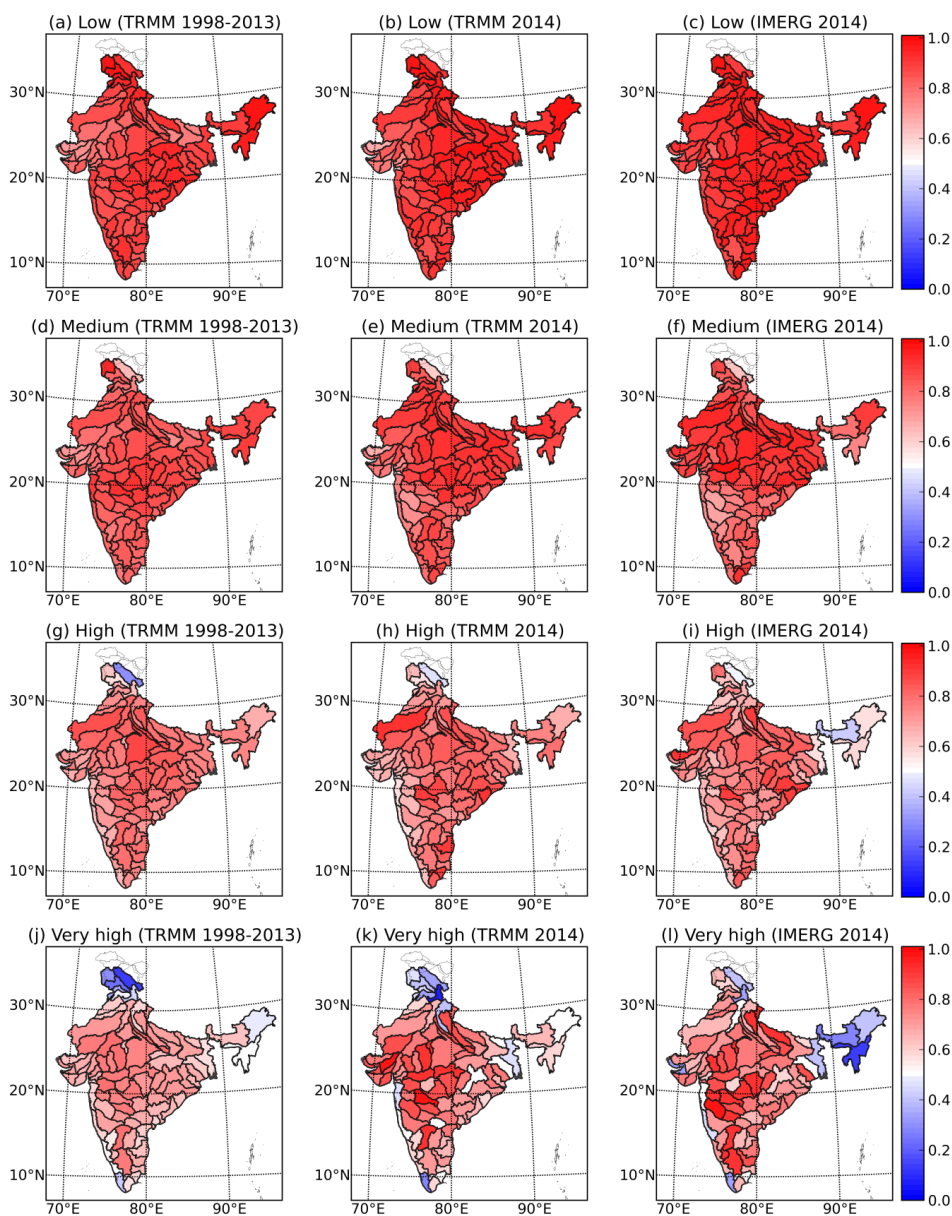
752

753 **Figure 5.** Percentage bias of TRMM (1998-2013), TRMM (2014) and IMERG (2014) over
754 86 major basins in India for (a) overall time series and over (b) low, (c) medium and (d) high
755 rainfall regime.



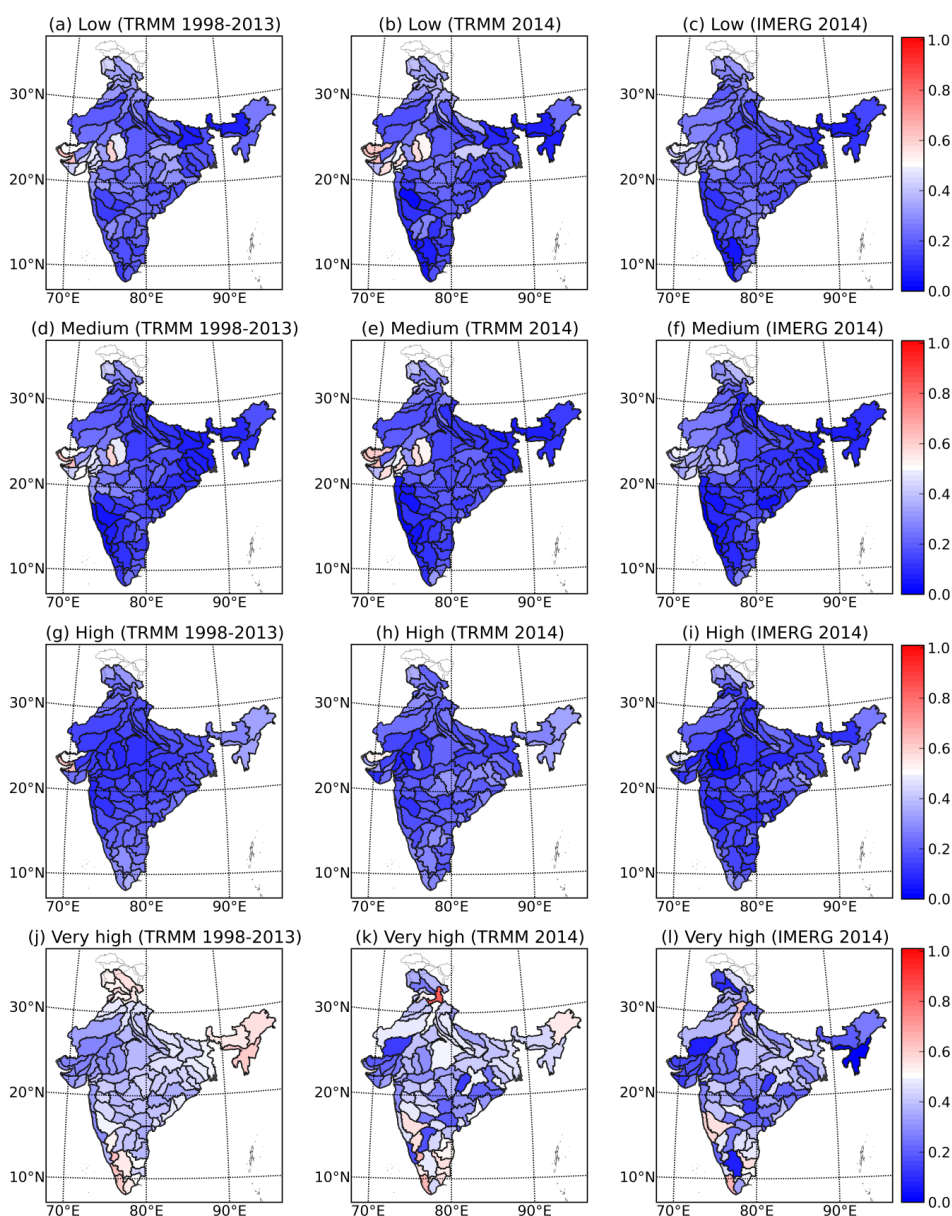
756

757 **Figure 6.** Spatial representation of percentage bias of TRMM (1998-2013), TRMM (2014)
758 and IMERG (2014) over 86 major basins in India for (a) – (c) overall time series and over (d)
759 – (f) low, (g) – (i) medium and (j) – (l) high rainfall regime.



760

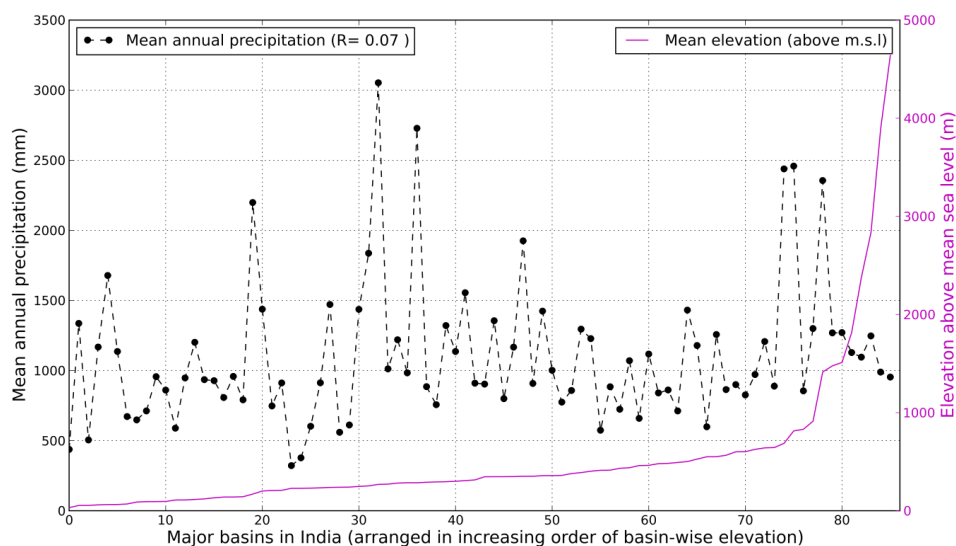
761 **Figure 7.** Spatial representation of probability of detection (POD) for (a) – (c) low (25
762 percentile), (d) – (f) medium (50 percentile), (g) – (i) high (75 percentile) and (j) – (l)
763 very high (95 percentile) rainfall threshold for TRMM (1998-2013), TRMM (2014) and IMERG
764 (2014) rainfall estimates over 86 major basins in India.



765

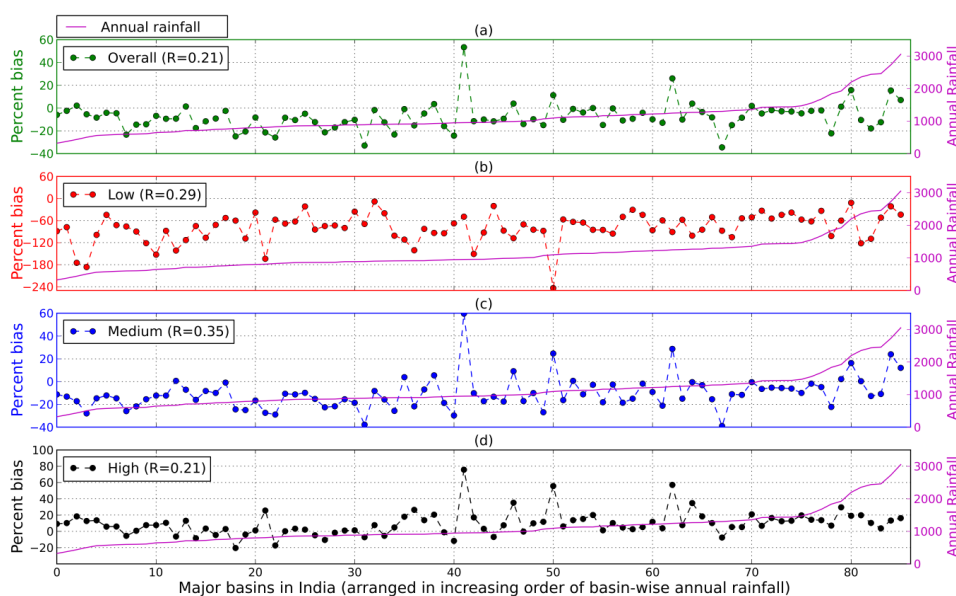
766 **Figure 8.** Spatial representation of false alarm ratio (FAR) for (a) – (c) low (25 percentile),
 767 (d) – (f) medium (50 percentile), (g) – (i) high (75 percentile) and (j) – (l) very high (95
 768 percentile) rainfall threshold for TRMM (1998-2013), TRMM (2014) and IMERG (2014)
 769 rainfall estimates over 86 major basins in India.

770



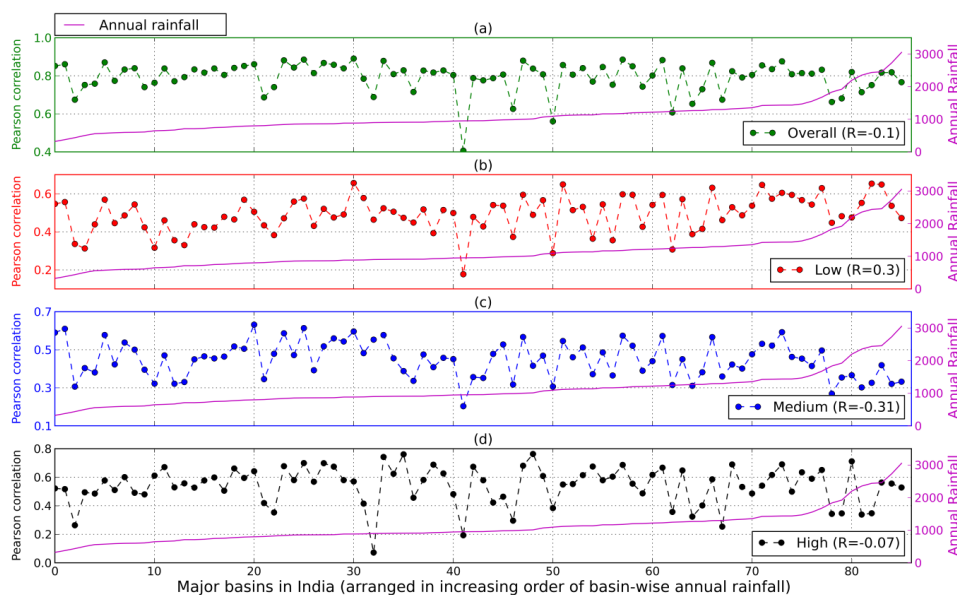
771

772 **Figure 9.** Graphical representation of long term average annual rainfall (calculated from IMD
 773 gridded rainfall dataset from years 1980-2010) and average elevation above mean sea level
 774 for 86 major basins in India (arranged in increasing order of their mean elevation).

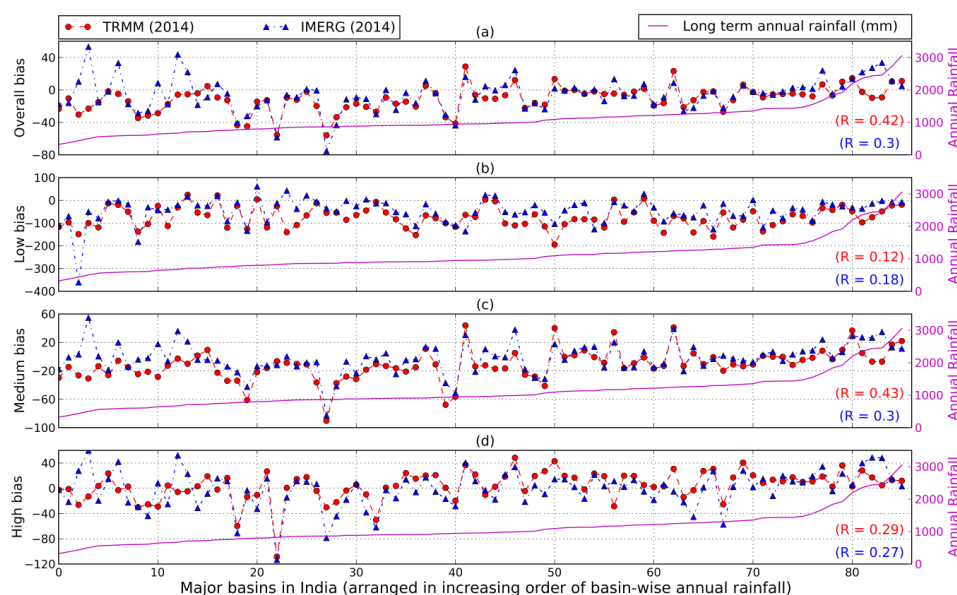


775

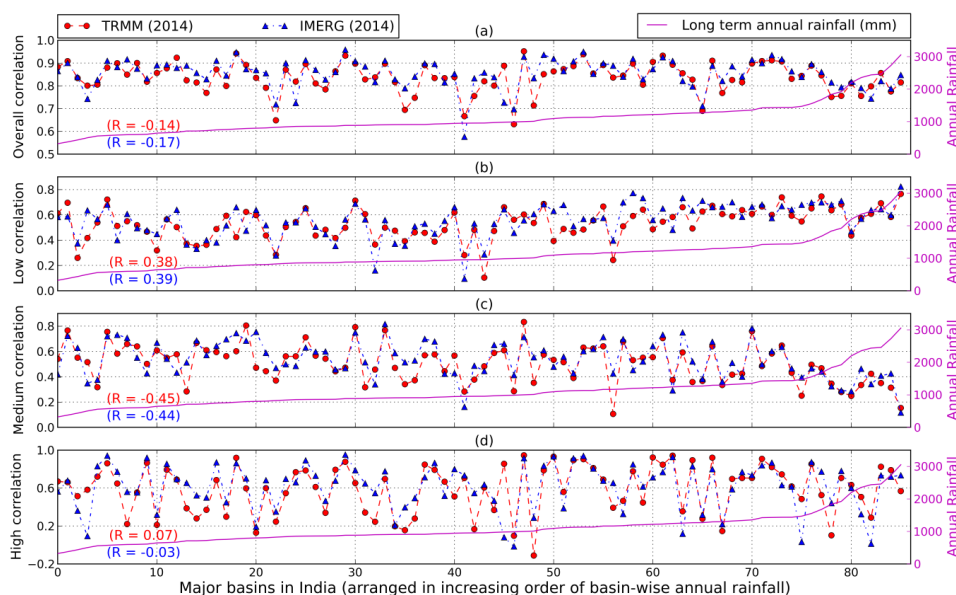
776 **Figure 10.** Graphical representation of percentage bias of TRMM (1998-2013) arranged in
 777 the increasing order of basin-wise average annual rainfall for (a) overall time series and over
 778 (b) low, (c) medium and (d) high rainfall regime for 86 major basins in India.



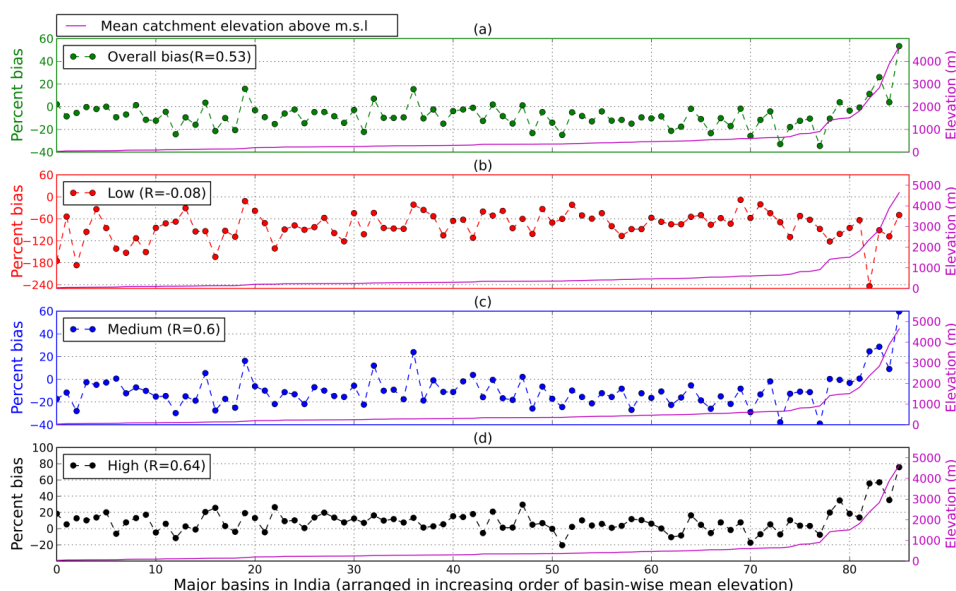
779
 780 **Figure 11.** Graphical representation of correlation of TRMM (1998-2013) arranged in the
 781 increasing order of basin-wise average annual rainfall for (a) overall time series and over (b)
 782 low, (c) medium and (d) high rainfall regime for 86 major basins in India.



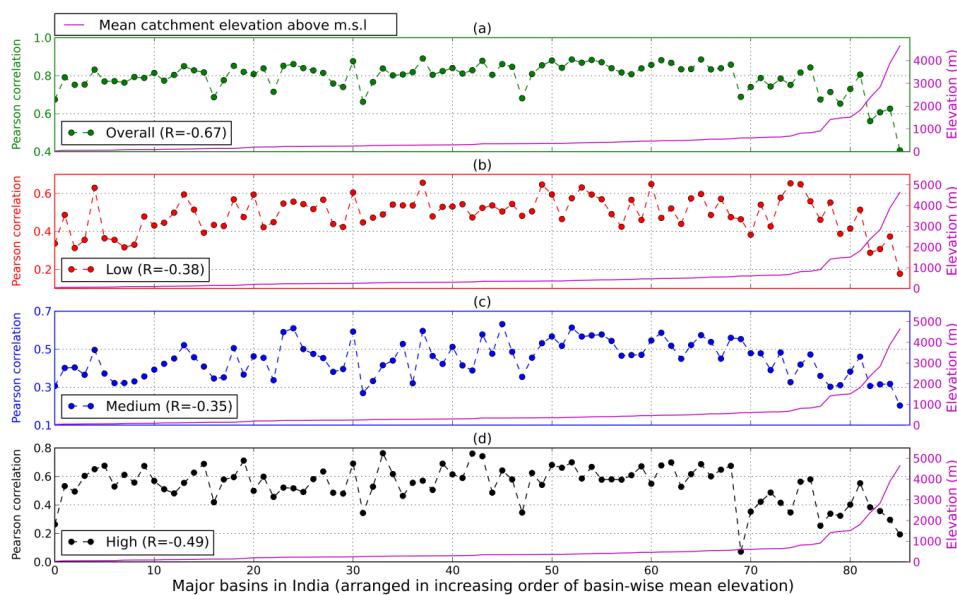
783
 784 **Figure 12.** Graphical representation of percentage bias of IMERG (2014) and TRMM (2014)
 785 arranged in the increasing order of basin-wise average annual rainfall for (a) overall time
 786 series and over (b) low, (c) medium and (d) high rainfall regime for 86 major basins in India.



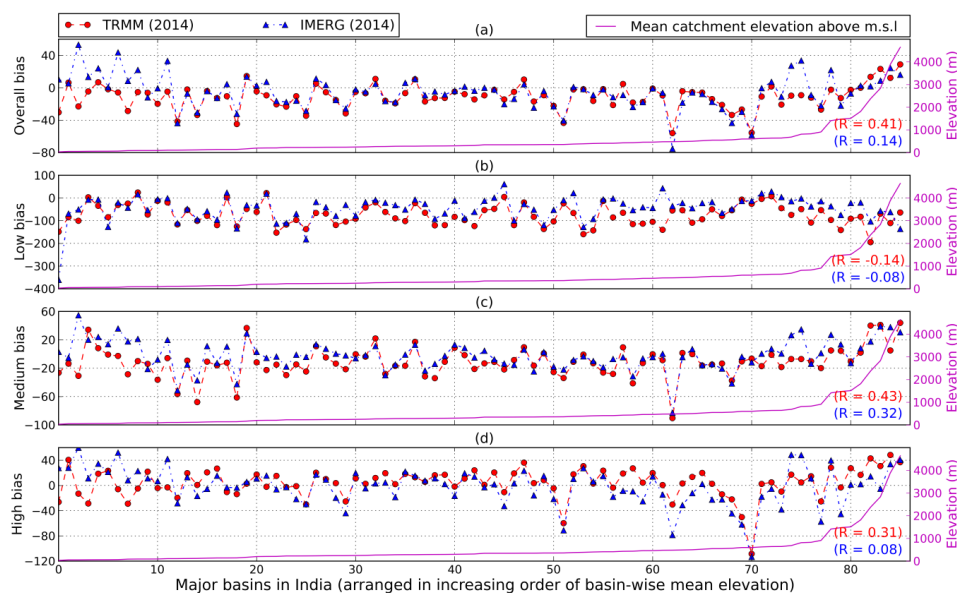
787
 788 **Figure 13.** Graphical representation of correlation of IMERG (2014) and TRMM (2014)
 789 arranged in the increasing order of basin-wise average annual rainfall for (a) overall time
 790 series and over (b) low, (c) medium and (d) high rainfall regime for 86 major basins in India.



791
 792 **Figure 14.** Graphical representation of percentage bias of TRMM (1998-2013) arranged in
 793 the increasing order of basin-wise average elevation over mean sea level for (a) overall time
 794 series and over (b) low, (c) medium and (d) high rainfall regime for 86 major basins in India.



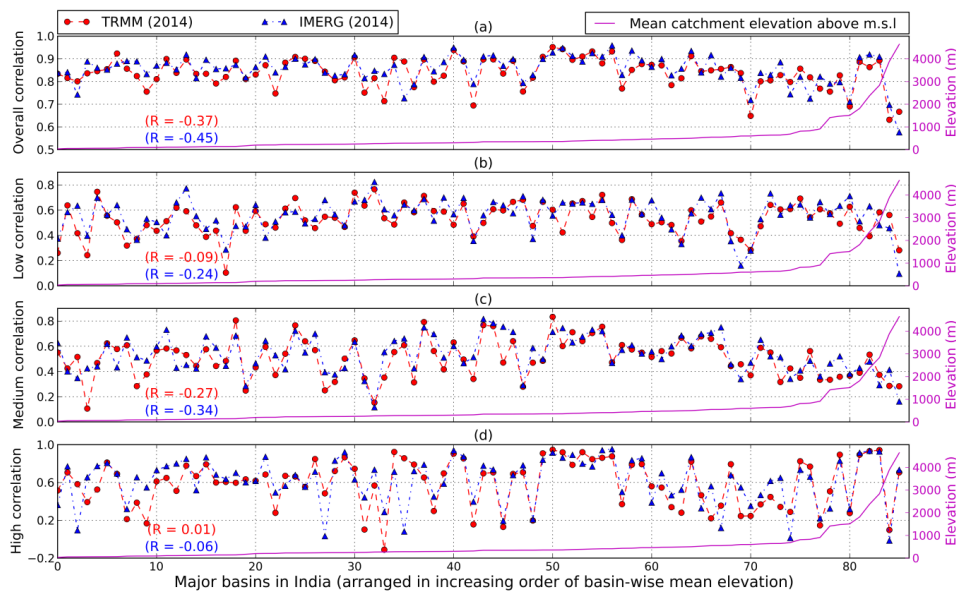
795
 796 **Figure 15.** Graphical representation of correlation of TRMM (1998-2013) arranged in the
 797 increasing order of basin-wise average elevation over mean sea level for (a) overall time series and over (b) low, (c) medium and (d) high rainfall regime for 86 major basins in India.
 798



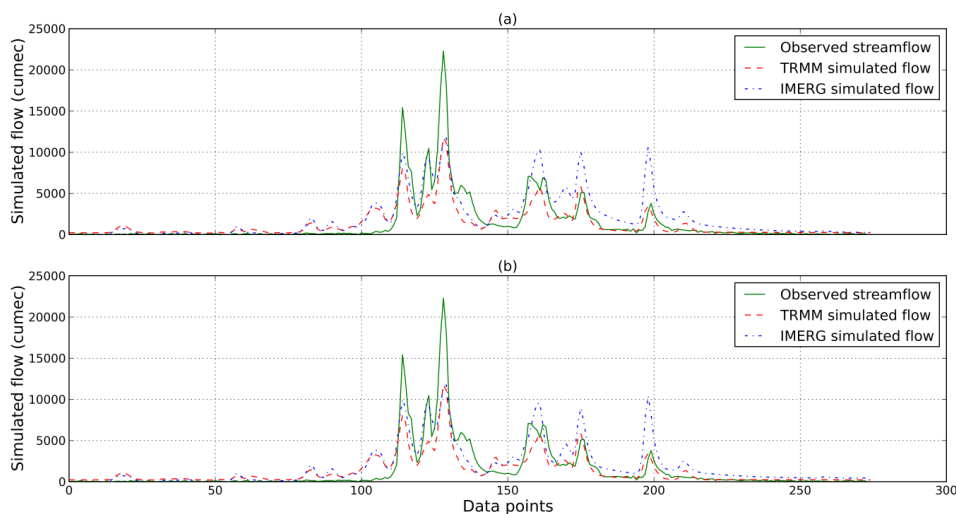
799
 800 **Figure 16.** Graphical representation of percentage bias of IMERG (2014) and TRMM (2014)
 801 arranged in the increasing order of basin-wise average elevation over mean sea level for (a)



802 overall time series and over (b) low, (c) medium and (d) high rainfall regime for 86 major
 803 basins in India.



804 **Figure 17.** Graphical representation of correlation of IMERG (2014) and TRMM (2014)
 805 arranged in the increasing order of basin-wise average elevation over mean sea level for (a)
 806 overall time series and over (b) low, (c) medium and (d) high rainfall regime for 86 major
 807 basins in India.
 808



809



810 **Figure 18.** Hydrographs for TRMM and IMERG simulations (April 1, 2014 – December 31,
811 2014) with (a) IMD and (b) TRMM calibrated VIC model.



812 **Table 1.** Summary of the precipitation datasets used.

Product name	Spatial resolution	Temporal resolution	Spatial coverage	Temporal coverage	Period used in this study
IMD Gridded Rainfall	0.25° x 0.25°	Daily	Indian landmass	1901-2014	1998-2013, 12 th March, 2014 – 31 st December 2014
TRMM Research product	0.25° x 0.25°	3-hourly	50° N-S	1998-present	1998-2013, 12 th March, 2014 – 31 st December 2014
IMERG Final Run	0.1° x 0.1°	Half-hourly	60° N-S	12 th March, 2014 – present	12 th March, 2014 – 31 st December 2014

813 **Table 2.** Contingency table used to calculate probability of detection (POD) and false alarm

814 ratio (FAR) at a given rainfall threshold.

		Simulated	
		> Threshold	<= Threshold
Observed	> Threshold	HIT	MISS
	<= Threshold	FALSE	NEGATIVE

815 **Table 3.** Summary of different statistical indices used to evaluate the satellite precipitation

816 products.

Index	Formula	Best value	Worst value
Pearson correlation (R)	$\frac{\sum(X - \bar{X})(Y - \bar{Y})}{\sqrt{\sum(X - \bar{X})^2} \sqrt{\sum(Y - \bar{Y})^2}}$	1	0
Percentage bias (Pbias)	$\frac{\sum(X - Y)}{\sum X} * 100$	0	$+\infty / -\infty$
Probability of detection (POD)	$\frac{HIT}{HIT + MISS}$	1	0
False alarm ratio (FAR)	$\frac{FALSE}{HIT + FALSE}$	0	1
Nash Sutcliffe efficiency (NSE)	$1 - \frac{\sum(X - Y)^2}{\sum(X - \bar{X})^2}$	1	$-\infty$ (negative value means that mean is a better estimator)



			than the model).
Root mean squared error (RMSE)	$\sqrt{\frac{\sum(X - Y)^2}{n}}$	0	$+\infty$

817 ($X = Observed, \bar{X} = Observed\ mean, Y = Simulated, \bar{Y} = Simulated\ mean, n =$
 818 $Data\ points$)

819 **Table 4.** Segregation of overall rainfall time series into low, medium and high rainfall time
 820 series ($R = Rainfall, \mu = Mean\ of\ rainfall, \sigma = Standard\ deviation\ of\ rainfall$).

Rainfall regime	Criterion
Low	$R < \mu$
Medium	$R \geq \mu$ and $R \leq \mu + 2\sigma$
High	$R > \mu + 2\sigma$

821 **Table 5.** Performance statistics for rainfall-runoff modeling using VIC for Hirakud catchment
 822 of Mahanadi River basin in India.

	Time period	NSE	R^2 (p-value)	P-bias	RMSE (m^3/s)
IMD calibration	2000-2011	0.83	0.84 (0.01)	-16.78	919.88
IMD validation	2012-2014	0.86	0.88 (0.01)	-3.91	823.58
TRMM calibration	2000-2011	0.72	0.74 (0.01)	-18.2	1160.94
TRMM validation	2012-2014	0.73	0.74 (0.01)	-14	1128.15
TRMM (IMD calibration)	2014	0.72	0.82 (0.01)	9.41	1591.09
IMERG (IMD calibration)	2014	0.64	0.68 (0.01)	-41.4	1786.22
TRMM (TRMM calibration)	2014	0.72	0.82 (0.01)	9.24	1588.86
IMERG (TRMM calibration)	2014	0.7	0.72 (0.01)	-31.32	1641.82

823